This article has been accepted for publication in IEEE Transactions on Transportation Electrification. This is the author's version which has not been fully edited and content may change prior to final publication. Citation information: DOI 10.1109/TTE.2023.3321707

Automotive Electric Propulsion Systems: A Technology Outlook

Babak Fahimi, *Fellow, IEEE*, Laura H. Lewis, *Fellow, IEEE*, John M. Miller, *Life Fellow, IEEE*, Steven D. Pekarek, *Fellow, IEEE*, Ion Boldea, *Life Fellow, IEEE*, Burak Ozpineci, *Fellow, IEEE*, Kay Hameyer, *Senior Member, IEEE*, Steven Schulz, *Member, IEEE*, Ahmad Ghaderi, *Member IEEE*, Mircea Popescu, *Fellow, IEEE*, Bradley Lehman, *Fellow, IEEE,* Dhruvi Dhairya Patel, *Student Member, IEEE*

***Abstract*— Electrification of the transportation industry introduces far-reaching paradigm shifts in sustainability, energy dependency, and manufacturing sectors. The ultimate success of this transition, in part, depends on sustainable development of highly efficient, reliable, and affordable electric propulsion systems. This article provides an overview on the existing practices and future trends in magnetic design, power electronic converter, and control/safety for electric propulsion systems. Efficiency, torque density, cost, noise and vibration, and reliability are used as figures of merit in this study. Our investigation identifies the areas of research with the highest impact and the highest urgency. Although several challenges have been identified, these areas all provide great opportunities for future research in this emerging industry.**

***Index Terms*— Efficiency, Motor Drives, Power Electronics Propulsion, Reliability.**

I. INTRODUCTION

Electrification of the transportation industry is one of the most impactful transformations of our time. It is bringing profound changes into the energy sector and will undoubtedly affect climate change, geopolitical balances, and the sustainability of existing resources. This paradigm shift will revolutionize generation, distribution, and consumption of electricity by incentivizing massive use of non–fossil fuel sources of electricity, reinventing distribution grids and assessing new modes of wired and wireless charging infrastructure, on-route charging via electrified highways, as well as other applications of dynamic wireless charging. Although passenger cars have been the primary target of the early phase of electrification, off-road vehicles, trains, airplanes, and ships will soon follow this fast-growing trend. Figure 1 illustrates the anticipated compound annual growth rate (CAGR) in the automotive electric propulsion motor market within the next few years [1]. Although the demand follows an exponential trajectory, the ultimate success of this transition will depend on reliable development of highly efficient, compact, affordable, and fault tolerant electric propulsion units and regenerative energy storage systems with attendant uni/bidirectional chargers. The electric propulsion unit consists of the traction inverter, electric motor/generator, and potentially a transmission system. This article aims to provide an in-depth overview of the state-of-the-art and future trends in the design and development of automotive electric propulsion motors and their accompanying power converters.

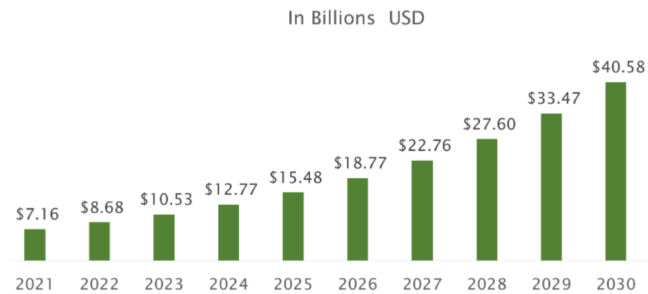

Fig. 1. CAGR for EV motor market.

II. SYSTEM OVERVIEW

Transition from internal combustion engines and liquid fuel to an electric vehicle (EV) platform introduces several fundamental components, including a power electronic converter, electric propulsion motor, onboard charger, auxiliary DC-DC converter for non-propulsion loads, thermal management system, and battery storage unit. Figure 2a shows a generic placement of these components within an EV. Notably, in hybrid, battery, and fuel cell EVs, different sources of energy and energy converters are necessary. However, the electric propulsion system, as illustrated in Figure 2b, is a common denominator among all hybrid, battery, and fuel cell EVs. The electromechanical conversion of energy takes place in the airgap of electric machines and therefore deserves

Corresponding author: Babak Fahimi. Babak Fahimi is with the University of Texas at Dallas, Richardson, TX 75080 USA (email: fahimi@utdallas.edu), Laura H. Lewis is with the Northeastern University, Boston, MA 02115 USA (email: lhlewis@northeastern.edu) , John M. Miller is with J-N-J Miller design services PLLC, Kilgore TX 75662 USA (email: jmmiller35@aol.com), Steven D. Pekarek is with Purdue University, West Lafayette, IN47907, USA(email: spekarek@purdue.edu), Ion Boldea is with Timisoara Polytechnique, Timisoara, Romania (email: ion.boldea@upt.ro), Burak Ozpineci is with ONRL, Oak Ridge, TN 37830, USA (email: burak@ornl.gov), Kay Hameyer is with RWTH-Aachen, Aachen, Germany (email: hameyer@iem.rwth-aachen.de), Steven Schulz is with Rivian, Irvine, CA92606, USA (email: sschulz@rivian.com), Ahmad Ghaderi is with DANA corporation, Novi, MI 48377, USA, (email: ahmad.ghaderi@dana.com), Mircea Popescu is with Ansys Corporation, Wrexham, UK (email: mirceap@ieee.org), Brad Lehman is with Northeastern University, Boston, MA 02115, USA (email: lehman@ece.neu.edu), Dhruvi Dhairya Patel is with the University of Texas at Dallas, Richardson, TX 75080 USA (email: dhruvi.patel2@utdallas.edu).

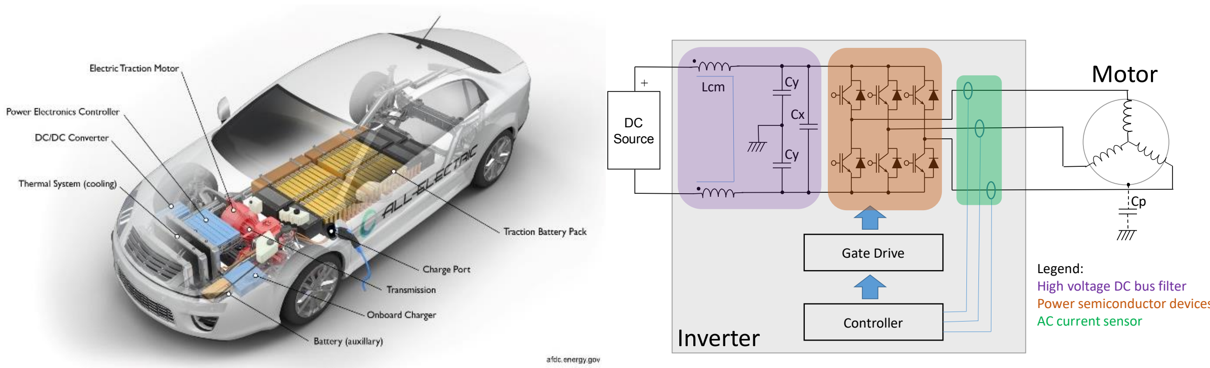

(a) (b)

Fig. 2. (a) Fundamental components of an electrified vehicle, and (b) electric propulsion system.

significant attention. Equally important is the power converter, which alters the form of electric energy to optimally match the needs of the electric motor/generator. Among various forms of energy conversion, mankind has mastered the art of efficient bidirectional electromechanical energy conversion and this development alone gives a winning edge to electric propulsion systems. Efficiency of motor drive systems is typically provided as a single number, which is the efficiency at the rated operating point. However, the actual running efficiencies of a motor and an inverter vary depending on the operating point. Figure 3 shows the loss and efficiency maps of a 2016 BMW i3 traction inverter and motor, and their combined drive efficiency [2]. If the probability p of operating at an arbitrary point in the torque-speed plane for a given driving scenario is given by $p(\omega, T)$, then the running efficiency η_{run} of the electric propulsion system can be approximated using the expression

$$\eta_{run} = \iint \eta_{con}(\omega, T).\eta_{mot}(\omega, T).p(\omega, T)d\omega \cdot dT \quad (1)$$

where the integration is performed over the entire torque-speed range of the drive system.

In this article, state-of-the-art and future trends of development for electric propulsion systems are discussed. Electric motors are discussed first, followed by power converters, and finally control and safety protocols. The main purpose of this article is to highlight accomplishments and challenges as we move toward an all-electric transportation industry.

III. Electric Machines

In electric propulsion systems, a conversion from electrical to mechanical energy (and vice versa) within a magnetic medium (*i.e.*, an electric motor) takes place. For the limited cluster of magnetic configurations envisioned to date, impressive performances have been captured. However, given current unoptimized usage of the material, wasteful arrangement of magnetic forces and non-ideal thermal performance, propulsion motors require much more research. This section summarizes the existing magnetic configurations, materials, and challenges in electric machines.

A. Materials

The specific choice of traction motor type for battery EVs is influenced by numerous factors, including cost, volume, weight, durability, starting torque, speed range, reliability, maintenance, noise, vibration, and harshness (NVH) requirements. Ehsani *et al.* [3] compared features of five of the most widely used electric machines for EV and hybrid EV applications—there are the brushless DC motor, the series DC motor, the permanent magnet (PM) synchronous motor, the switched reluctance motor, and the AC induction motor. These motor types all exhibit a variety of advantages and disadvantages that depend on the specific combination and arrangement of magnets contained within the coupled electrical power input to linear or rotary output and consequent motion. The performance of these magnets has been undergoing optimization since the beginning of the 20th century through precise materials engineering from the atomic to the centimeter scale of the bulk magnet itself. However, the fundamental nature of the atoms that comprise these essential materials prevents simultaneous optimization of all engineering performance metrics, so OEMs must work with end users to determine acceptable performance trade-offs. The overarching goal to minimize traction motor weight and size while maximizing performance requires the use of the highest-grade magnets available to manufacturers. This section provides an overview of existing high-performance magnets and discusses motivation and progress regarding the development of next-generation magnets necessary to support the 21.26% projected CAGR in electrified mobility [4].

1) **Motors and magnets**

Electric traction motors operate via the interaction of electromagnetic components to generate torque that is applied to the motor shaft. These components comprise a magnetic circuit that can contain two categories of magnets: hard (permanent) magnets and soft magnets [5]. Hard magnets store appreciable energy per unit volume and exhibit a high coercivity, or resistance to demagnetization, to provide strong magnetic alignment in rotor poles. In contrast, soft magnets are designed to store only minimal energy and ideally exhibit a very small resistance to

This article has been accepted for publication in IEEE Transactions on Transportation Electrification. This is the author's version which has not been fully edited and content may change prior to final publication. Citation information: DOI 10.1109/TTE.2023.3321707

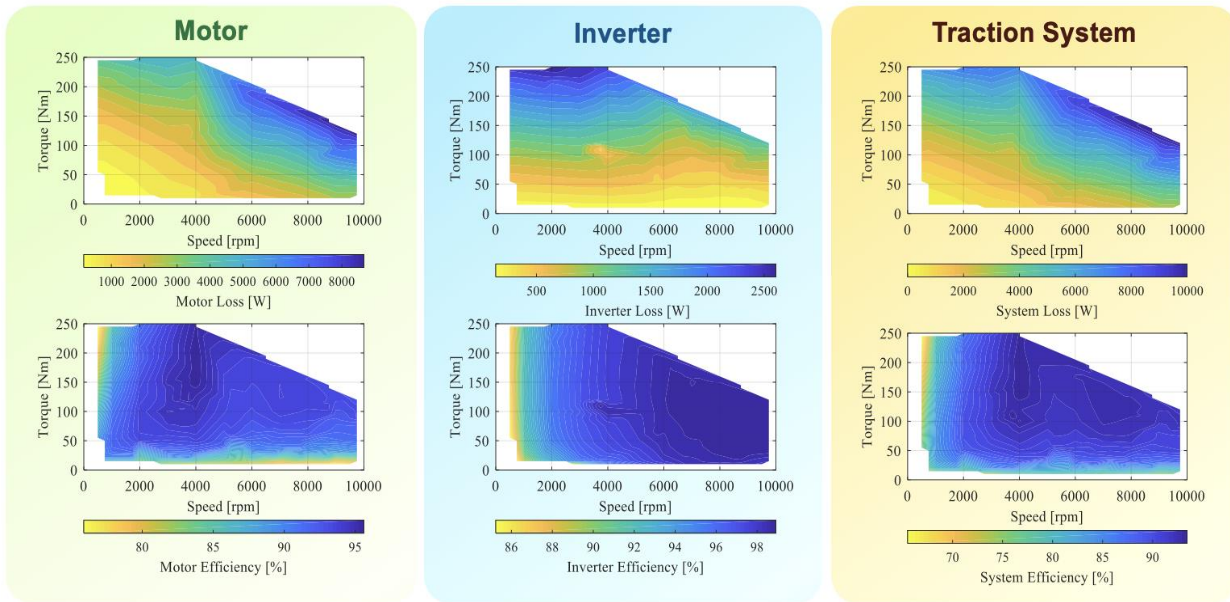

Fig. 3. Experimental loss and efficiency data plots for a 2016 BMW i3 traction drive.

magnetic reversal, enabling fast and efficient reversal of polarity. Although electric machine architects typically seek to combine the strongest available hard magnets with the lowest-coercivity soft magnets within their designs, nature and/or geopolitics can hinder these plans. The traction motor landscape is subjected to dynamic trade-offs and compromises regarding magnet choices. For example, in 2017, it was revealed that the electric propulsion of recent Tesla models includes a PM electric motor in addition to the induction motor used in all prior Tesla models [6].

2) **Choices, challenges, and aspirations for high-performance hard magnets**

High-performance rare earth (RE) magnets are the overwhelmingly preferred choice for traction motor designers who prioritize low weight and small size. These ultra strong "super magnets," which can store a large amount of energy in a minimized volume [7], [8], are made from intermetallic compositions characterized by highly complex crystalline networks of Fe and/or Co—to provide the large magnetization—that contain interspersed light RE atoms such as Nd, Pr, and Sm at a level of approximately 32 wt. % to provide high coercivity via a strong quantum-mechanical spin-orbit coupling at the atomic level. A small concentration of boron or Ti provides stability to the crystal structure, and the addition of heavy RE elements such as Dy or Tb (up to 10 wt %) amplifies the coercivity, especially at the elevated operating temperatures of most traction motors. RE elements possess unique electronic structures, and direct atomic substitutions do not exist. Because of sourcing issues (*e.g.*, cost and availability), the distribution of heavy REs such as Dy and Tb has been reduced, with efforts to localize them to boundaries of crystallites that make up the magnet rather than within these crystallites.

Although RE magnets have many advantages, intrinsic shortcomings include excessive brittleness derived from strong intermetallic atomic bonding, which creates difficulty in machining and poor mechanical robustness in high-frequency motors. Recent studies show that losses in RE magnets are caused by both eddy current and hysteresis. One study state, "The results indicate that the hysteresis loss resulting from the structural imperfections and geometry of the magnet may introduce a considerable loss in NdFeB PMs applied in rotating electrical machines" [9]. Furthermore, RE magnets have a strong propensity to oxidize, which severely degrades performance. Although traction motor engineers consistently seek magnets with increased saturation magnetization, increased coercivity, and improved high-temperature performance, these attributes are ultimately limited by the behavior of the specific atoms and thus cannot be further optimized, motivating new electrical system designs. Also, supply limitations of RE elements and magnets create challenges for OEMs and end users. This scenario—a repeat of the so-called "rare-earth crisis" [10] of 2011, which resulted in 3,000-fold price spike in Dy and a 5,000-fold price spike in Tb [11]—motivated manufacturers to seek strategies to significantly reduce the amount of Dy added to NdFeB magnets without sacrificing performance [12]. The current version of the RE crisis may be attributed to various new factors, including changing geopolitics, economic and environmental considerations, geological realities, climate change concerns, domestic workforce depletion, and the COVID-19 pandemic. The United States has taken strong steps to develop domestic production (including recycling), increase workforce development, and secure critical material supply chains to meet sustainable energy and domestic security targets [13]. These actions are accompanied by recent US participation on behalf of ANSI

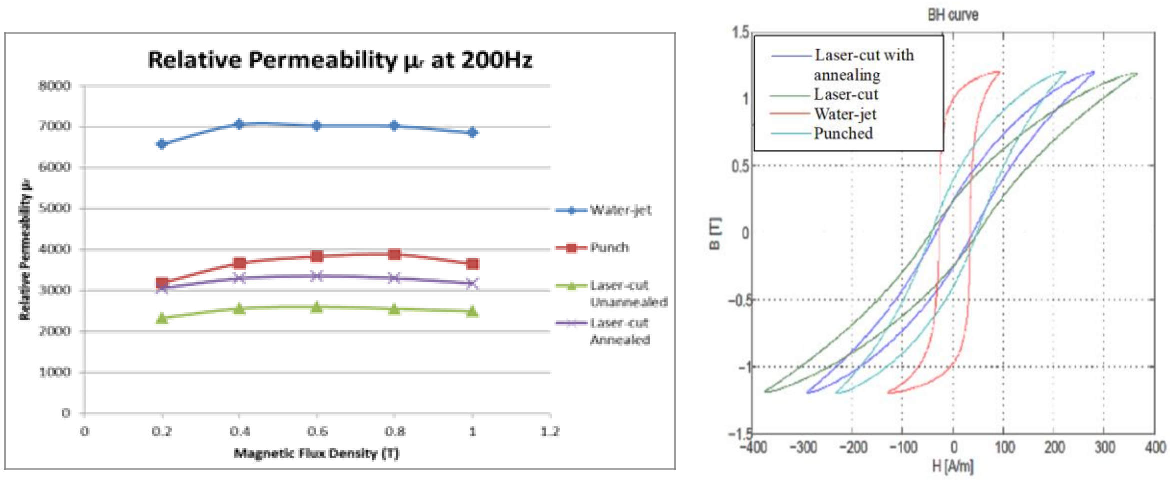

(a) (b)

Fig. 4. Changes in permeability (a) and hysteresis loop (b) caused by various methods of production for lamination.

in ISO (International Standards Organization)/TC (Technical Committee) 298 Rare Earths, which seeks to develop international standards in RE mining, concentration, extraction, separation, and conversion, as well as recycling of useful RE compounds/materials, which are key inputs to manufacturing and furthering production processes in a safe and environmentally sustainable manner. In addition to developing additional RE resources and magnets, efforts are underway to create strong PMs containing minimal to zero RE content. This task requires designing chemical bonds at the atomic level to approximate the electronic role of the RE element. Additionally, because the energy density of a PM is determined by intrinsic and extrinsic factors (such as constituent crystallite size and arrangement), realization of practical alternatives to RE super magnets necessitates careful engineering at the nano- and micron scales as well. Alternatives to RE magnets do exist, but they currently lack a sufficient energy density to replace RE magnets and are therefore better suited as “gap magnets” [14] that possess a stored energy intermediate between weak oxide magnets and RE magnets. Many of these compounds have been known for decades, but interest in their development faded when compounds based on RE elements were discovered [8], [15], [16], [17]. Although this class of intermediate-strength magnets can reduce pressure on the RE magnet supply, thus freeing them for the most critical applications, novel motor topologies must be developed for these useful but lower-performance magnets.

3) Choices, challenges, and aspirations for efficient soft magnets

Efficient transfer of energy in electrical machines requires soft magnetic materials with high-saturation magnetization and good magnetic permeability coupled with very low coercivity to enable easy polarization reversal [18]. Furthermore, soft magnetic materials must exhibit good electrical resistivity to minimize losses. To this end, performance trade-offs must be made when incorporating electrical insulation that reduces eddy current losses but also dilutes the magnetic induction. Additionally, soft magnetic materials must possess good mechanical strength and be easy to manufacture.

The current soft magnet market mainly comprises electrical steels [18] in inexpensive isotropic forms and more expensive grain-oriented forms. Although electrical steels are well suited for the low excitation frequencies (<1 kHz) of conventional electric machines [19], [20], high-speed traction motors for electric and hybrid vehicles require fundamental frequencies above 1.5 kHz [21]. These requirements necessitate improved alloys with higher flux density and lower losses at elevated frequencies to enable new types of electrical systems [22], [23].

The chemical elements that comprise silicon steels mainly Fe and Si, are among the most abundant elements in the Earth’s crust and thus are not subjected to supply constraints as RE elements are. Therefore, the main routes toward realizing improved soft alloys are enhanced control of the alloy structure and the parallel development of more efficient manufacturing approaches, rather than new alloy compositions. Because magnetic properties originate at the atomic scale, the soft magnet alloy structure must also be controlled at this level to influence these properties. To address this need, engineers have developed strategies to rapidly cool molten magnetic alloys at a very high rate (up to millions of degrees per second) to capture the atomic structure of the liquid alloy but retain it in the solid state [24]. These subtle but highly important atomic rearrangements allow for significantly improved soft performance but donate a lowered magnetic induction. Nonetheless, these amorphous/nanocrystalline soft magnet alloys are highly desired for high-frequency devices, including power converters and electrified mobility vehicles. Formed into wide, very thin (tens of microns)

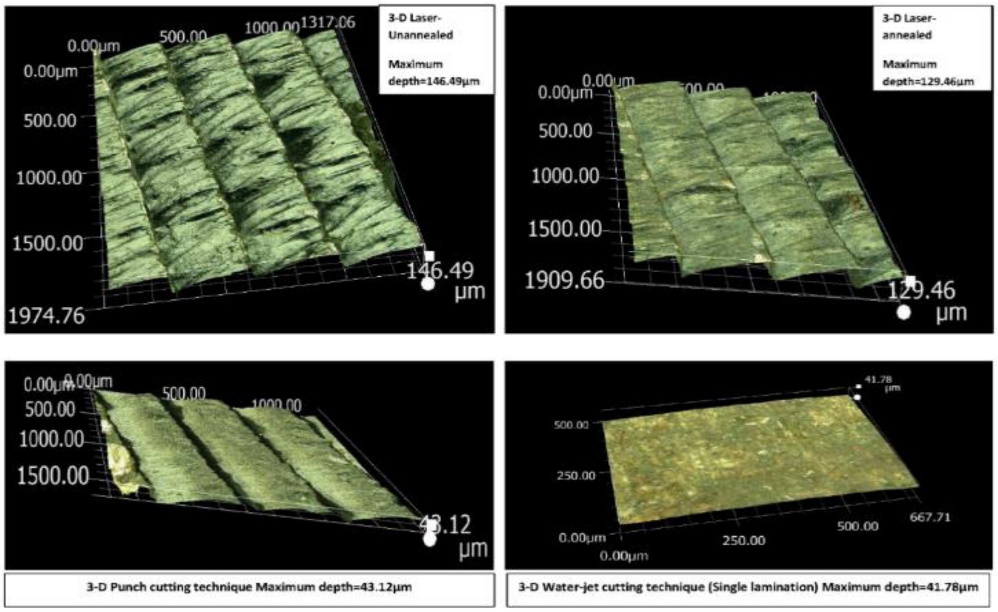

Fig. 5. Surface smoothness in M-19 laminations cut using various techniques.

sheets, advanced soft magnetic alloys are typically subjected to low-temperature thermal treatments to drive minute atomic motions that relieve strain, reduce losses, and customize the magnetic response [25], [26]. In addition to the requirement for better understanding and control of these thermal treatments, other pressing manufacturing challenges include development of the necessary alloy nano/microstructure without sacrificing mechanical integrity and innovating methods to transform the soft magnet sheets into complex shapes required by certain motor topologies. Additive manufacturing techniques show significant promise in this area [27], [28] and will require continued optimization.

Manufacturing processes are crucial in the overall performance of motors. Figure 4 shows an experimental comparison between magnetic properties of M-19 laminations that have been prepared using four different methods: water jet cutting, laser cutting with and without annealing, and die-punching. The extreme thermal and mechanical stresses introduced by laser cutting and die-punching compromise the structure of the magnet crystals close to the airgap (i.e., the most sensitive area in energy conversion) and deteriorates the relative permeability and core losses of the material. In contrast, water-jet cutting has a minimal impact on material properties. Although changes in permeability may not introduce a major effect on machines' working inductances, the accompanying hysteresis loss increases do have a measurable effect on torque density and efficiency of electric machines, and especially in reluctance electric machines.

Furthermore, as motor designers seek higher power densities, especially in reluctance machines, motivation exists to reduce the airgap. The cutting mechanism employed to create the laminated alloy introduces limitations on the airgap size. Figure 5 shows images of M-19 laminations that were created using various cutting techniques. The water-jet cutting method provides imperfection sizes of about 40 µm, in sharp contrast to those produced by laser cutting, which introduces imperfections of diameters 130–145 µm. Inconsistencies in the airgap can lead to substantial deterioration in performance and may increase torque pulsation and magnetically excited audible noise.

B. Performance Metrics

1) **Torque Density**

Electric machines used in applications such as traction motors for light- and heavy-duty passenger vehicles put a premium on package size and mass. Consequently, the operation of these motors is typically tuned to a specific application; the torque and speed zones that experience highest use are given priority in terms of performance and efficiency. This prioritization generally leads to electromagnetic designs specifying magnetic flux and current loops with the shortest and least obstructive paths. In the following examples of electromechanical converters, magnetic couplings have torque densities around 100 N·m/L and specific powers above 20 kW/kg; magnetic gears (MGs) have similar properties, and motor-generators have torque densities around 50 N·m/L and specific powers up to 10 kW/kg with forced air cooling, and yet higher with liquid cooling such as a 50/50 water-ethylene glycol solution. Magnetic devices that possess the highest gravimetric (N·m/kg) and volumetric (N·m/L) torque densities belong to the class of PM couplers (PMCs) [29] for radial and axial PMC construction. PMC devices have applications in areas that are not suitable for mechanical shaft ports and require non-contacting transmission of torque, such as chemical mixers and pumps. Figure 6 provides examples of both axial and radial PMC

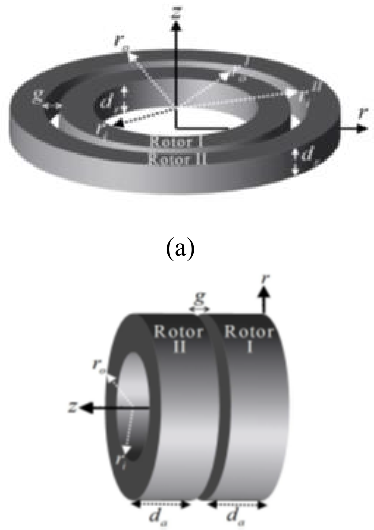

(a)

(b)

Fig. 6. Radial (a) and axial (b) PMCs.

constructions. Li *et al*. [29] note that PMC torque density is dependent on six parameters inherent to a dual annular structure: these are the outer radius r_o of the outer annular structure; the inner radius r_i of an inner annular structure; the airgap, *g* between these annular structures ;also a mid-gap radius r_g, axial length d_r; and pole pairs *p*. They found that the peak torque density always occurs under the conditions $r_g = \frac{r_o+r_i}{2}$, radial magnet thickness $t_m = \frac{r_o-r_i-g}{2}$ and $r_o - t_m = \frac{p t_m \pi}{4}$. One may note that, r_g represents a lever arm for torque, t_m is a measure of the permanent magnet mass, and $r_o - t_m$ is the back iron (yoke) mass. Furthermore, radial PMCs have higher torque density than axial PMCs. A radial PMC may have torque density above 1,000 N·m/L and specific torque of 200 N·m/kg. This sizing methodology is applicable to motor generators.

Around 2001, magnetic coupling was applied to magnetic gears that were capable of non-unity speed ratios and possessed inherent non-contacting torque transfer, very low noise, good wear resistance, and overload protection. The radial PMC structure in MGs with magnetic coupling now includes PMs (or slots and windings) on its outer structure with PMs located on, buried in, or, as found in Halbach arrays, positioned on the outer surface of the inner structure along with an expanded airgap housing a ferromagnetic flux modulator with an integer (preferably even) number of segments (i.e., poles) in which all three rotors are free to rotate. Figure 7 shows the basic magnetic gear with three concentric rotors. The component is conceptually similar to an epicyclic (*i.e*., planetary) gear consisting of an outer ring, *R*, inner sun, *S*, and interposing planet gears on a carrier, *C*. The relationships between the number of rotor teeth in the epicyclic gear may be described as in Eq. 2:

$$N_s + kN_r - (1+k)N_c = 0 \tag{2}$$

where $N_s, N_r, and\ N_c$ represent the number of gear teeth for sun, outer ring, and carrier respectively. Uppalapati *et al*. [30] demonstrated that for magnetic gears,

$$p_1\omega_1 = n_2\omega_2 - p_3\omega_3 \tag{3}$$

where p_1 is the number of pole pairs of the inner structure, n_2 is the number of modulator segments, and p_3 is the number of pole pairs in the outer structure. They noted that the outer and inner rotors with PMs interact with the middle rotor that possesses n_2 ferrous poles to produce harmonics in space. If the relationship between poles is selected as $p_1 = |n_2 - p_3|$, then the rotors interact via a common space harmonic, and Eq. (3) is satisfied. In this case the gear ratio can be expressed as $G_r = \frac{n_2}{p_1}$, where $n_2 = p_1 + p_3$ or the sum of the number of pole pairs of the outer and inner rotors.

A magnetic gear can achieve a volumetric torque density T_m of 100 N·m/L with typical air-cooled mass torque densities of 10–15 N·m/kg. As an example, a MG of $p_1 = 4$ pole pairs, $n_2 = 17$ and $p_3 = 13$ pole pairs has a gear ratio of 1:4.25 from w_1 to w_2, with $w_3 = 0$. The torque level in this case (?) is estimated to be 85 N·m with 98.5% efficiency using RE magnets.

A unique application for magnetic gears is in the propulsion unit of electric aircraft [31], where a high-speed electric motor drives the inner (*S*) rotor to extract high torque at lower speed from the middle (modulator) rotor with the outer p_3 rotor grounded. Figure 8 shows an MG proposed for aircraft electrified propulsion applications in which a high-speed electric machine drives an inner Halbach array rotor composed of four magnet segments per pole pair. The outer rotor consists of p_3 pole pairs, each of which is also a four-magnet segment array.

The prototype MG unit with the structure $p_1 = 2$, $n_2 = 26$

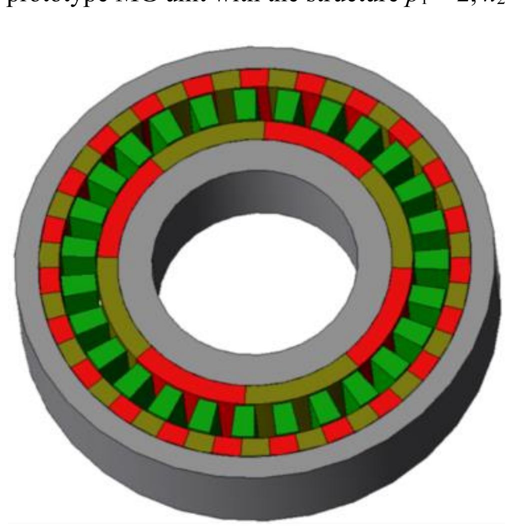

Fig. 7. General structure of an MG.

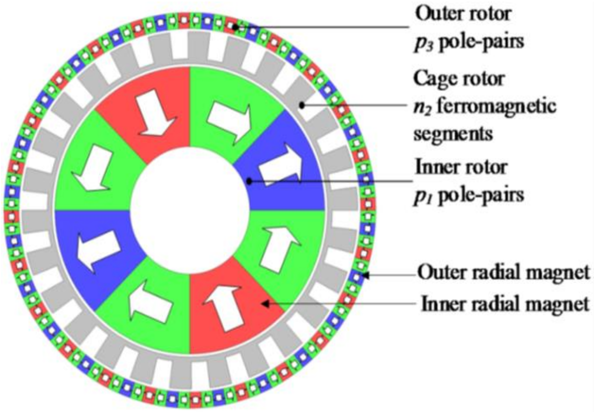

Fig. 8. Integrated MG in an aircraft application.

and p_3 = 48 has G_r = 13 and inner radius r_i = 86 mm, r_{io} = 99.5 mm and r_o = 111 mm with stack length of d_r = 25 mm, allows a mass torque density T_m = 53.4 N·m/kg. Three-dimensional end effects cause the actual T_m to be well below calculated values of 95 N·m/kg and 248 N·m/L. However, these performance estimates for PMCs and MGs do provide valuable insight into the limits on mass and volumetric torque density that can be achieved in practical machines using RE magnets.

Ley and Lutz [33] discussed electric propulsors for an electric aircraft that demonstrated specific power of 13 kW/kg employing a cantilevered outer rotor of Halbach array magnets, a slot-less inner stator, an integrated heat sink, and forced air cooling. This prototype had a specific power of 24 kW/kg when considering only active mass. The electrified propulsor motors exhibited 97% efficiency using Cu conductor coils and forced air cooling. With liquid cooling and higher current density in the conductors, specific power higher than 20 kW/kg and 98% efficiency were achieved.

Ley and Lutz [33] also noted that motors containing superconducting coils have the potential to realize specific power densities >50 kW/kg and efficiencies >99%. The challenge to create slot-less superconducting coil motors is a need to incorporate form-wound coils that can withstand high normal and shear forces without deformation. Magnetic frequencies (dB/dt) in excess of 5,000 T/s will be encountered in slot-less synchronous PM machines, and using superconducting coils increases this value by 3 to 4 times. Designing the stator coil structure to withstand extreme normal and shear forces, as well as designing cryocooling systems, remain the main challenges for the realization of superconducting motors.

The PMC, MG, and superconducting aircraft motors discussed allow expanded contemplation of what is feasible in EV and aircraft propulsion motors. To date, the designs of most EV traction motors contain inner-rotor-buried magnets that develop torque as the combination of magnet and reluctance contributions. Safety concerns restrict the interior PM synchronous motor (IPMSM) for EVs to a weak-magnet, high–reluctance ratio design. Because of the magnetic saturation characteristics of motor-grade steels, the reluctance, (or saliency) L_d/L_q is nominally 2:1 in strong-magnet IPMSMs and is approximately 2.5:1 in reluctance-dominated IPMSMs [33]. Ley and Lutz [33] described the development of a U-shaped buried-magnet IPMSM that meets the US Department of Energy (DOE) Freedom CAR goal of 55 kW peak power, 2.7 kW/kg specific power, and 14.3 N·m/kg torque. Considering only an electromagnetic mass of 40.5 kg and volume of 3.5 L, the active metrics are power density of 16.2 kW/L and torque density of 77.3 N·m/L.

These authors selected a 12-pole IPMSM with 3 slots per pole, and a U-shaped buried-magnet rotor. The demonstrated saliency ratio of this design is 1.48. The torque of IPMSM is given by Eq. (4), where T_e is the average electromagnetic torque, p is number of the pole pairs, φ_m is the flux linkage due to PMs, I_d and I_q are the direct and quadrature axis currents in the rotor frame of reference, respectively, and L_d and L_q are the inductances in the direct and quadrature axis respectively.

$$T_e = \frac{3p}{2} I_q\left(\varphi_m + (L_d - L_q) I_d\right) \tag{4}$$

The US Freedom Car goals call for traction motors with 55 kW peak, 30 kW continuous power at < 400 A_{rms} per phase, with an open-circuit voltage limit of below 60 V/krpm for safety. Ley and Lutz' proposed design achieved metrics of L_q = 111 mH, L_d = 75 mH, n_b = 2,000 rpm, n_{mx} = 10,000 rpm, and a maximum torque of 262 N·m. Because the IPMSM requires only 1.007 kg of RE magnets, it yields utilization metrics of 55 kW/kg(per kg of PM) and 262 N·m/kg_(per kg of PM). The electromagnetic design with 36 slots, 12 poles, and 3 phases was novel in that its slot/pole/phase (SPP) ratio value of unity translated to a winding factor of k_w = 1.0 and satisfied short flux and current loops. The saliency ratio of 1.48 is typical of IPMSM designs, especially under load when the quadrature axis inductance L_q experiences saturation. The U-shaped rotor magnets contributed to larger inner rotor space.

As a point of reference, the 2010 Toyota Prius 60 kW IPMSM provides a specific power of 77 kW/kg_(per kg of PM) and a torque of 268 N·m/kg_(per kg of PM). Prior to focusing on high-performance IPMSMs, researchers at DOE's Oak Ridge National Laboratory investigated integer- and fractional -lot PM synchronous motors (PMSMs). Bailey and McKeever [34] summarized these efforts and provided detailed designs and modeling guidance applicable to IPMSMs. A recent IPMSM innovation involves use of a rotor employing a hybrid design of spoke-type flux-concentrating PMs combined with a Halbach array [35]. This design exhibited a high saliency ratio along with high torque and power density.

A hybrid-rotor IPMSM [36] achieved a PM-specific torque of 168.6 N·m/kg_PM, torque density of 108 N·m/L, and specific power of 4.78 kW/kg. Under the condition of

200 A, the IPMSM developed a torque of 217N.m arising mainly from the magnets, and a rated power of 58 kW. Considering a reasonable saliency ratio of 1.45, the reluctance torque was only 10% of the total torque after extracting L_d = 201.6 µH and $\varphi_m = 0.1\ Wb - turn$, making it a strong-magnet IPMSM. The application to automotive starter-alternator duty drives the requirement of an overall package dimensions limited to 260 mm outer diameter and approximately 50 mm length. This is very similar to the rating of the IPMSM described by Coey [5], which reached a PM-specific torque of 262 N·m/kg_PM.

Torque density serves as a dependable metric to assess the electromechanical productivity of electric motors. However, in the automotive context, incorporating power density and specific power inherently considers the influence of operating speed. Notably, higher operating speeds lead to more compact motors for a given power output. This is the underlying reason for the use of transmission in electric drivetrains. Leveraging the high efficiency and industrial maturity of transmissions has proven instrumental in substantially reducing the size of traction motors and inverters. Yet, this advantage comes at the trade-off of operating at higher voltages and requiring reinforced insulation.

2) **Efficiency**

Permanent magnet couplers and magnetic gear designs can deliver efficiencies greater than 98.5%, with that of slot-less outer-rotor PM motors exceeding 97%. The use of superconducting coils in the proposed aircraft electrified propulsor motor [31] allows achievement of efficiencies in excess of 99%, making it quasi-adiabatic. Even so, at power ratings of 1 MW and higher, the heat rejection is still around 10 kW for such MGs that are proposed as a gearbox replacement. Clever electromagnetic designs utilizing short and tight flux and current loops in IPMSMs could increase efficiency values to around 97% while achieving very high magnet utilization metrics in the 200 N·m/kg_PM regime [29].

While the inclusion of advanced thermal management designs facilitates higher electric machine performance, efficiency gains become much more costly, especially when efficiency exceeds 95% and moves towards 97%. Advances in superconducting coils and in high-temperature superconductors, as noted by Ley and Lutz [33], make this efficiency possible but at high complexity and cost, along with the challenge of cryogenic plumbing and coolants.

Bomela *et al*. [37] discussed the impact of various material compositions in MG applications and demonstrated that the use of soft magnetic composites, instead of electrical steels, made little difference in the attained levels of torque and efficiency. As expected, the use of RE magnets instead of ferrite magnets demonstrated four times higher output torque and power.

The main reason why PM machines of any design possess high efficiency is the magnetization of the working gap by the magnets. The magnetization of PM machines is derived by "pre-paid" permanent magnets and thus is considered as a capital cost, whereas that of induction machines (IMs) and switched reluctance machines (SRMs) is derived from an external source and is thus an operating cost. Consequently, IMs and SRMs have inherently lower efficiency, and they place a higher reactive VA (volt-ampere) burden on the drive inverter.

3) **Fault Tolerance**

High–torque density electric machines incorporate robust stator structures and are made using precise manufacturing processes. The rotor, whether it is cantilevered, an outer runner, or uses an inner runner, introduces robustness concerns that are primarily mechanical. Surface PM machines, in which permanent magnets are attached to the circumference of the rotor, benefit from outer runner designs such as those employed in aircraft propulsors but suffer in terms of bearing structures. Inner-rotor surface PM machines require reinforcement to maintain the surface magnets in place against high centrifugal and magnetic forces. Magnet retainers such as carbon fiber wrap or mylar help this situation but also increase the magnetic gap, which then requires the use of thicker magnets. Induction machines containing cast aluminum or copper rotors may experience fractures, especially of the end rings, that contribute to torque pulsation and eventual machine breakdown. IPMSM rotors face the most stringent mechanical retention demands because of the required bridges and post structure. The incorporation of two U-shaped bridge permanent magnets into successfully met performance targets [33]. Later incarnations designed to further enhance magnetic performance, such as incorporation of a flux-focusing spoke combined with a Halbach magnet array rotor, experienced serious structural integrity issues during operation. In addition, the possibility of demagnetization at the high temperatures realized in PM machines is a concern.

Fault tolerance requirements are pervasive and include all electrical, magnetic, mechanical, and thermal aspects of a given electric machine design. The earliest electric machine exhibiting superior fault tolerance was the SRM consisting of double saliencies of stator slots for windings and rotor teeth to achieve high levels of reluctance variation [38]. However, this design required a small airgap because of the large magnitude of the turning force, $F_t = (1 / \mu_0) * B_n B_t$, where B_n is the normal directed flux density and B_t is the tangential component. This large turning force is proportional to B_n^2 and deforms the SRM stator resulting in structural impairment and excessive noise. These factors underlie why SRMs have not been quickly adopted in traction and propulsor motors. Still, SRMs have outstanding fault tolerance because of little or no mutual flux between phases, which can be three or larger. Because SRMs do not contain permanent magnets, they are economical and have excellent service life. In the past

Fig. 9. Double stator SRM configuration.

decade, double stator SRMs have been introduced (Figure 9), which have high torque density [35].

4) **Sustainability**

The selection of electric traction motors must align with sustainability principles, encompassing economic, manufacturing, environmental and durability considerations. With the increasing demand for RE in offshore wind generators, electrified automotive and aerospace propulsion systems, and other industries, ensuring affordability in accessing RE presents a genuine challenge for economic sustainability in the years ahead. Moreover, supply chain issues related to RE procurement can further impact production costs.

Over the past decade, fluctuations in the price of Neodymium Oxide and Dysprosium have been tolerated by car manufacturers. However, given the projected demand for the next decade, these volatile prices may pose economic sustainability concerns. Notably, the recycling of RE in electric motors remains uncommon, with many manufacturers preferring to use new RE, leading to potential environmental concerns.

From an environmental vantage point, it is notable that extraction of one kilogram of neodymium oxide will release 30.2 kg of CO_2 into the atmosphere, while the similar figure for silicon steel, copper, and aluminum is 3.5, 6.7, and 6.67 kg CO_2/kg respectively [36]. This comparison illustrates the notable negative impact of rare earth extraction and processing on pollution and environmental quality.

Finally, the possibility of demagnetization and permanent damage of the electric propulsion unit can introduce a new question on the effective lifetime and durability of the RE magnet-based motor drives. A complete life cycle analysis including raw materials extraction and processing, development of parts, manufacturing the motor, operation, and end-of-life recycling under the stochastic and volatile conditions of each stage is deemed necessary.

All indicators suggest that reliance on RE magnet-based electric propulsion units in a dominantly electrified automotive industry will face sustainability issues. Similar concerns can be raised for power electronic converters that require printed circuit boards, passive elements, and power electronic modules. Overall, the environmental impact of this growing global industry needs close attention. For example, design and realization of modular motor drives that are easy to dissemble for recycling purposes is of the highest importance.

It is all but certain that economic affordability and environmental concerns will force the industry to adopt a more active recycling strategy for raw materials. Similarly, new choices for electric propulsion motors such as wound-rotor synchronous machines will be examined as the concerns over continued use of permanent magnet-based devices has posed serious concerns. Singly excited motors such as induction and switched reluctance machines offer less complexity and higher robustness when compared to brushless wound rotor synchronous machines, attributes that can promote their use in commercial and off-highway vehicles.

C. New Magnetic Configurations

The conflicting requirements of performance and cost indexes of electric propulsion motor drives necessitate novel

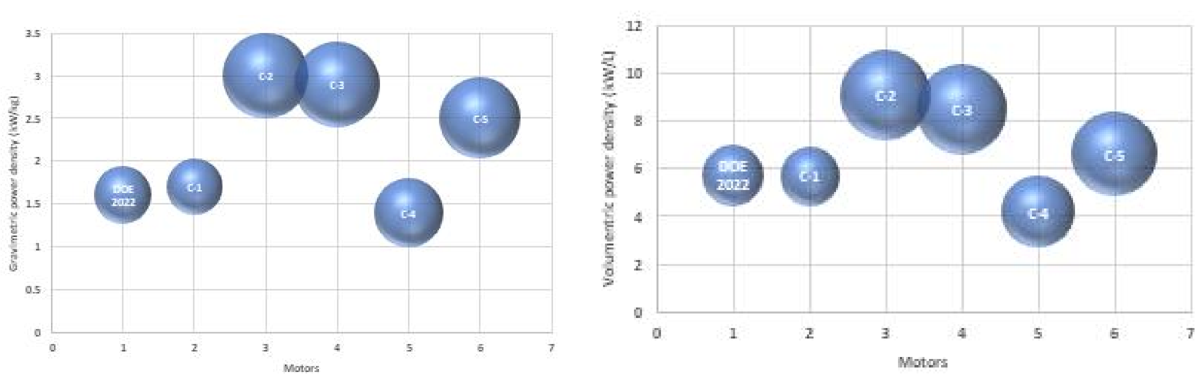

(a) (b)

Fig. 10. Gravimetric (a) and volumetric (b) power density of five commercially available propulsion motors along with DOE's 2022 targets.

This article has been accepted for publication in IEEE Transactions on Transportation Electrification. This is the author's version which has not been fully edited and content may change prior to final publication. Citation information: DOI 10.1109/TTE.2023.3321707

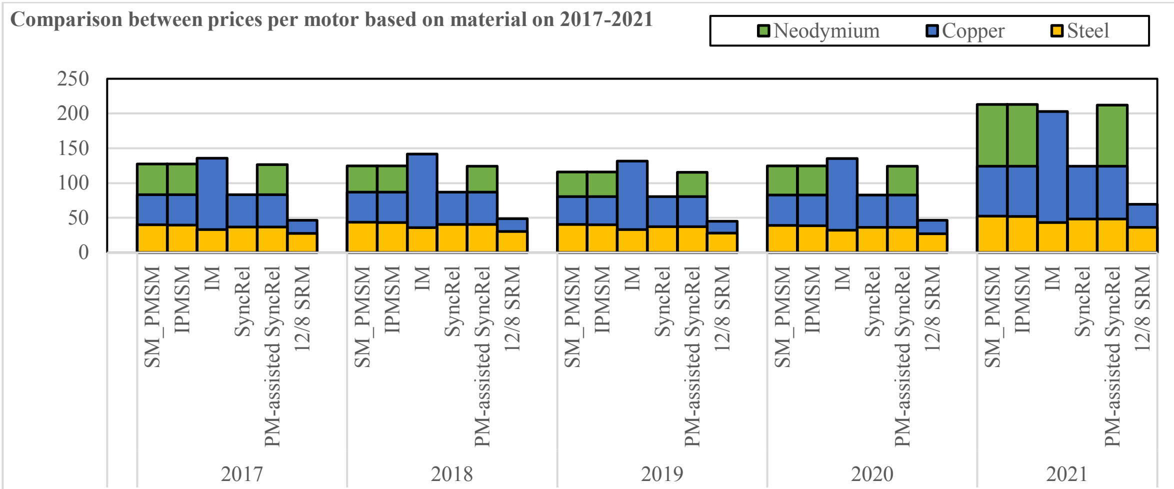

Fig. 11. Cost of raw material in surface-mounted PMSMs, IPMSMs, IMs, synchronous reluctance machines, PM-assisted synchronous reluctance machines, and switched reluctance machines at the same power and torque ratings.

designs and controls. Furthermore, the heavy duty that electric propulsion drives are exposed to donates unprecedented mechanical and thermal stress to the materials. To reach a compromise between high torque density, excellent efficiency, large power factor, and wide constant power speed ratio on one hand and manufacturing complexity, stringent cooling requirements, high cost of materials, and large system energy consumption on the other for a given design, novel electric machines have been sought. Geared and direct-drive systems have been used for various vehicles, but current focus is centered on high–torque density configurations using high-energy-density RE magnets and PM-free configurations with lower cost, despite their lower torque density.

Interior PM synchronous motors containing a V-shaped arrangement of high-energy-RE magnets are the primary choice for electric propulsion. High efficiency in the constant torque region, reasonable wide speed range in the constant power region, and impressive torque density are among the main merits of IPMSMs for electric propulsion. Figure 10 illustrates the gravimetric and volumetric power density of five leading commercial electric propulsion motors in comparison to DoE's 2022 targets (size of the circles represents their relative peak power). The use of transmissions results in exceeding both DoE targets with a tangible margin.

A comparison of the cost of raw material for various electric propulsion motor designs is illustrated in Figure 11. The cost of magnetic steel, magnetic wire, and RE magnets are the only factors in this comparison as the cost of end caps, shafts, cable leads, and bearings is nearly the same for all designs. This comparison was performed for a 250 kW, 6,000 rpm (base speed) motor. The sudden rise in the cost of RE magnets in 2011 illustrates a major leap in the cost of motor technologies in witch PMs are used. Also, the cost of Cu in SRMs with short end windings is among the lowest. As the price of RE magnets rises because of higher demand, less-expensive alternatives such as reluctance machines and IMs will gain attention.

Despite early success of IPMSMs, the increasing number of manufactured EVs and their outlook for coming years calls for alternative motors that more effectively use RE magnets (i.e., higher kilowatt/PM weight ratio), utilization of RE-free magnets, or altogether eliminate the use of magnets. The following design advances have had early success in achieving the described goals.

Axial flux arrangement for coils and RE PMs: Double-sided axial flux motors benefit from a larger airgap volume through which the rotating field of the stator and that of the surface mounted magnets interact. The axial forces tend to be strong and apply significant mechanical strain on the spacers that maintain the axial airgaps. The stack length of the machine tends to be short, which makes these electric machines an ideal choice for hub motors.

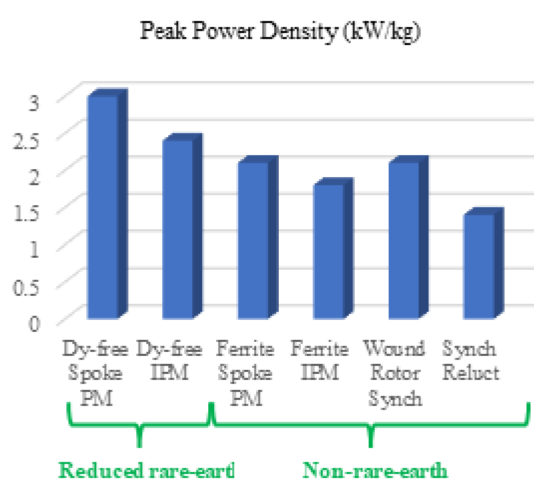

Fig. 12. Comparison of specific power between reduced RE and Non-RE motor technologies [38].

Tangentially magnetized PMs (spoke-type): Spoke motors with tangentially magnetized PMs have demonstrated substantial improvement in torque density. These machines in single- and dual-stator configurations can significantly increase the kilowatt/PM weight ratio. Therefore, ferrite and hybrid (e.g., ferrite/RE magnet) solutions have been used in these configurations. However, the ferrite magnets may cause demagnetization and lower torque density.

Wound rotor synchronous motor: Wound rotor synchronous motors with uniform airgaps and salient pole structures offer the closest substitute for permanent magnet motors. Clear advantages include absence of demagnetization, a controllable magnetizing power and removal of freewheeling losses without the need for a clutch. However, wireless transfer of power to the rotor winding seems to be a necessary addition as conventional brushes and slip rings will substantially increase the need for maintenance and may lead to safety concerns and longer length for the machine. It is also notable that removal of heat from the rotor, as reported in the case of induction motors, is an engineering challenge for wound rotor synchronous machines. Figure 12 shows a comparative study between motors with magnets made from reduced RE-content (i.e., Dy denotes Dysprosium) and zero RE content. As can be seen, wound rotor synchronous motors offer a very competitive specific power, a feature that has attracted the attention of several automotive manufacturers to consider this art of machinery as a viable alternate for IPMSM.

Synchronous reluctance and switched reluctance: Axially laminated synchronous reluctance machines and double stator switched reluctance machines have potential for application in electric propulsion systems [39], [40]. The very high saliency ratio in these alternatives enables competitive torque density. In general, reluctance machines have a lower efficiency than IPMSMs in the constant torque region, but they perform very competitively in the constant power region. With new advances in thermal management and the consequent increase in current density and filling factor, reluctance machines can be a reliable

a. Prius 2017 (Hairpin winding)

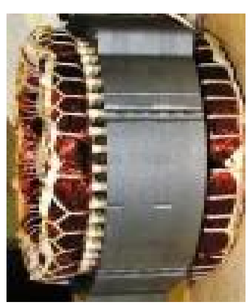

b. Prius 2010 random winding

Fig. 13. Hairpin winding and conventional random windings.

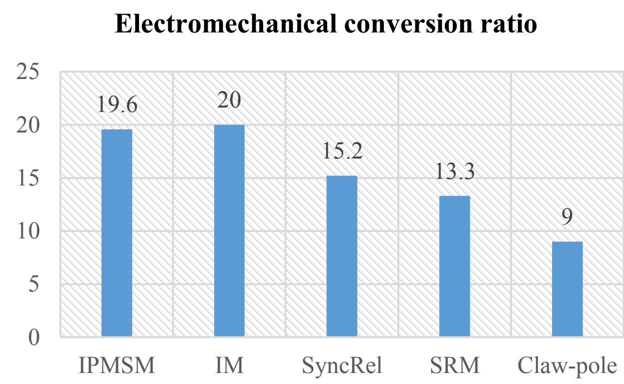

Fig. 14. Electromechanical energy conversion ratios.

alternative to IPMSMs. The short end winding in switched reluctance machines results in decreased usage of Cu, decreased losses, and a shorter stack length for the same effective magnetic length. Notably, the use of hairpin or single tooth winding results in short end windings, as well.

Induction motors: Squirrel cage induction motors have been used for electric propulsion by virtue of their brushless and robust design as well as the fact that they do not use RE-based permanent magnets. The power density and specific power of IM drives tend to be tangibly lower than those of IPMSM drives and closer to those of synchronous reluctance machines. Additional advantages of IM drives, which are made by well-established manufacturing practices, are low acoustic noise and vibration, and fault-tolerant operation. However, like reluctance machines, the magnetizing power of these drives must be provided by an inverter. Removal of excess heat from the rotor is not straightforward and needs relatively complex cooling arrangements. The efficiency of IMs is comparable to that of IPMSMs only in constant power region; additionally, IMs use significantly higher amount of copper .

Hairpin windings: In recent years the use of hairpin windings has reduced the amount of end coils as compared to conventional random windings that are used in the majority of AC adjustable-speed drives. Figure 13 illustrates the use of hairpin windings in the stator of a IPMSM in comparison to a random winding arrangement. The use of hairpin winding offers more efficient use of available space to deliver enhanced compactness. In [4] authors have demonstrated that the DC resistance of the stator phases can be reduced using hairpin windings. However, the AC resistance of these coils at higher operating speeds exceeds that provided by random windings. This phenomenon means that the efficiency of a particular motor depends on the effective speed of the propulsion drive. Notably the net reduction in amount of copper used in IMs is an important motivator in research and development of new winding configurations and manufacturing approaches.

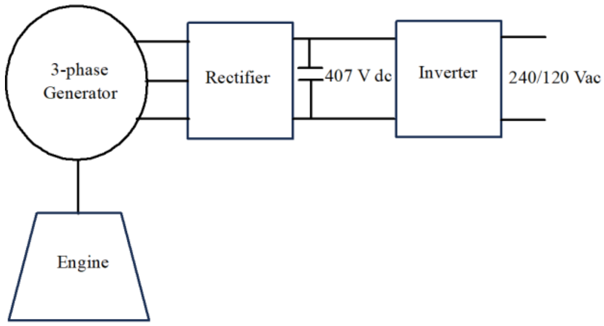

Fig. 15. Portable power system [44].

D. Optimization of Design

One approach for optimization of compactness is to examine the electromechanical energy conversion ratio σ, which can gauge the productivity of the overall energy conversion process. This metric is defined as the ratio of the net tangential forces acting on the rotor to the total sum of radial and tangential forces generated in the process over one electrical cycle:

$$\sigma[\%] = \frac{|F_t|}{|F_n|+|F_t|} \times 100 \tag{5}$$

Figure 14 illustrates this metric for five different types of conventional motors that were designed with the same geometrical envelope, filling factor, airgap length, and current density. Notably, the ratio of useful magnetic forces to total forces does not exceed 20% in any design, which suggests that common undesirable radial forces should be reduced while the tangential forces that contribute to useful mechanical work must increase.

With growing interest in electrified transportation, renewable energy systems, and alternative manufacturing technologies (e.g., 3D printing), the search for optimized electric machines and drive systems have dominated much of the electric machinery research over the past several years. Several recent reviews focused on machine/drive optimization; these include detailed descriptions of the optimization algorithms and open problems to explore [42], [43], [44]. Several recent books also describe the models and processes used to optimize machines, with a primary focus on multi-objective optimization [45].

A three-phase generator design described by Bash *et al.* [46], as shown in Figure 15, highlights the critical aspects of modern electric machinery optimization and how the process is evolving. Although this example does not directly target the design of an automotive electric propulsion motor, the principles of optimizations are identical. Notably, optimization of generators in series hybrid and regenerative braking through a separate electric machine can directly benefit from this case study. Bash *et al.* optimized a portable generator system similar to that used to provide backup power to homes and businesses. This system included an engine coupled to a 3-phase generator, a rectifier to convert the 3-phase generator AC voltage to DC voltage, and an inverter to convert the DC voltage to single-phase 120 V/240 V 60 Hz AC voltage. A key performance goal of this described system was portability, motivating minimization of generator mass. A competing design objective was to reduce power loss (*i.e.*, maximize efficiency) to minimize fuel consumption. Many candidates among electric machine architectures are able to convert engine-based mechanical power to 3-phase AC electromagnetic power. One of the most common designs is a wound-rotor synchronous machine (WRSM) that has a field winding to create the rotor magnetic poles. A second, less common design is a PMSM in which permanent magnets are used instead of a field winding. Similarly, there are alternative rectifier architectures that can convert the 3-phase generator AC output voltage to DC voltage. A key performance goal of the system was portability. architectures, design models were created for four candidates: PMSM with active rectifier (System I), PMSM with passive rectifier (System II), WRSM with active rectifier (System III), and WRSM with passive rectifier (System IV). These design models leverage analytical and magnetic circuit methods to compute the electromagnetic performance of candidate machines considering the geometric, excitation, and materials properties used to form the design space of each architecture. The size of the design space was specified, and 20 design parameters were considered for each system. Thermal aspects of the design were considered using current density limits of 7.6 A/mm^2 as a proxy for a thermally sound machine. Mechanical integrity was addressed using a maximum rotor tip speed of 180 m/s.

A modern electric machine design process leverages one of a host of optimization algorithms to perform rigorous multi-objective design. A key output of the optimization process is a Pareto optimal front, which represents a set of non-dominated designs that are all viable design options (*i.e.*, they will satisfy the required power, voltage, and any other specifications). Furthermore, a design in the set is characterized by the fact that alternative designs cannot outperform it in all performance objectives. To illustrate these points, the Pareto fronts for each of Systems I–IV (described in the previous paragraph) are shown in Figure 17. Considering the fronts individually, trade-offs between performance objectives (e.g., mass *versus* loss) for each system can be evaluated, and the effects of imposed efficiency requirements (or weight requirements) can be readily quantified. For example, for System I, lowering loss (*i.e.*, increasing efficiency) from 220 W (93.2%) to 140 W (95.6%) leads to more than a 200% increase in mass. Creating fronts for each machine architecture enables comparison of technologies and designs, such as PMSM versus WRSM systems. For the application in which portability was a significant factor, a PMSM provides the same efficiency as a WRSM at a fraction of the mass.

As computation and optimization resources and approaches have evolved, design interests have tended along several paths. A particular interest is in leveraging multi-physics (e.g., thermal, structural, electromagnetic) models within the performance evaluation of candidate machines/converters [45], [47], [48]. One study examined integration of different machine models to improve system performance, an approach motivated

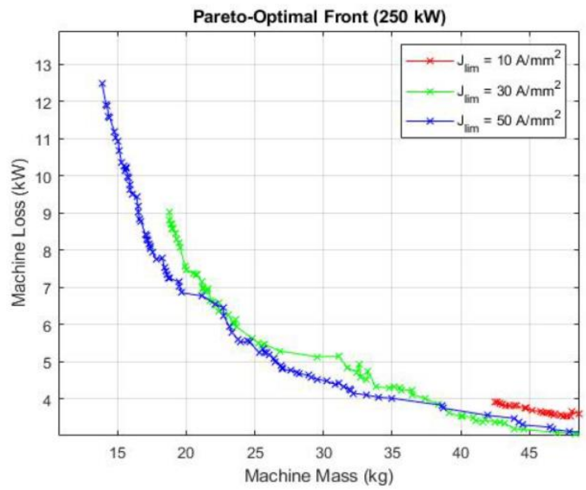

Fig. 16. Computed Pareto fronts for a radial flux PMSM with alternative cooling strategies enabling higher current densities.

by the US department of energy Aviation-Class Synergistically Cooled Electric-Motors with Integrated Drives program, which has a goal of advancing electric aircraft by dramatically improving the power density of the electric drives [49]. Specifically, the target requirements for this objective are to realize an all-electric propulsion drive of energy density greater than 12 kW/kg and efficiency greater than 93%. Recent research on the design of circuit board–based inductors with very high current densities [50] motivated a design study to consider increasing the current density of a standard radial flux surface-mounted PMSM, with the goal to achieve specified density and efficiency targets for a 250 kW, 5,000 rpm, 1-kV DC drive. Typically, current density limits for liquid-cooled machines are less than 30 A/mm^2 [51]. However, because SiC devices can be used to achieve stator excitation with high fundamental frequencies, thus enabling machine of the system (machine: 13.8 kg; inverter: 4.72 kg; coolant pump/components: 1.9 kg) was approximately 20.42 kg. A prototype of the winding/cooling system is being developed to validate this integrated model design approach.

The aviation class synergistically cooled electric motors with Integrated Drives program is motivated by a goal to electrify the transportation industry, which is key to realizing significant reductions in carbon-based emissions. Parallel efforts are being considered for ground vehicles, such as those publicized by DoE's Vehicle Technologies Office (VTO). A recent VTO announcement solicitated proposals to improve the power density and reduce the cost of 200 kW traction drives [52]. This program follows others that have focused on consideration of lower-power drives for passenger vehicles. However, a concern with widescale transportation electrification is that it will further compound environmental issues rather than reduce them. Of particular concern is that all components of machines, actuators, and charging infrastructure (e.g., Cu, steel, Al, magnet materials) have appreciable environmental costs associated with their production. Table I lists the energy requirements of the most common materials used in propulsion drives [53].

E. Reliability

Throughout the years, various factors have evolved in the development in electrical machines, including incorporation of faster switching devices, novel control techniques, and different types of mechanical loads (e.g., integrated transaxle) and their duty cycles. All mentioned components are electrically and/or mechanically connected to one another and operate under mutual interaction. In the past, converters, motors, and mechanical loads were treated and developed separately and then put in tandem to form the complete drive train. In contemporary applications, the system needs a holistic design approach so that the interactions among various components can be considered. In this new approach, even tolerances of the materials used or geometrical parameters and the influence of manufacturing processes on the single component must be considered as well.

It is necessary for researchers to consider what are the dominant drive train parameter(s) that describe an electric propulsion system to satisfy the requirements of high performance, high efficiency, reliability, and no radiated undesirable noise (e.g., RF, structural, airborne). To determine such parameters, a thorough analysis of the system must be performed that includes an in-depth examination of the physical behavior of the entire drive system (Figure 17).

The expected lifetime and reliability of an electric motor is dominantly determined by its winding insulation system and bearing condition. Insulation systems and their components

TABLE I
ENERGY REQUIREMENTS OF MATERIALS USED IN PROPULSION DRIVES

Material	Virgin manufacture		Recycled manufacture	
	Process energy per ton from virgin inputs (MMBtu)	Transportation energy per ton from virgin inputs (MMBtu)	Process energy per ton from recycled inputs (MMBtu)	Transportation energy per ton from virgin inputs (MMBtu)
Aluminum ingot	115.16	0.56	4.50	0.22
Steel	31.58	4.60	11.78	4.03
Copper wire	122.52	0.46	101.00	2.17

This article has been accepted for publication in IEEE Transactions on Transportation Electrification. This is the author's version which has not been fully edited and content may change prior to final publication. Citation information: DOI 10.1109/TTE.2023.3321707

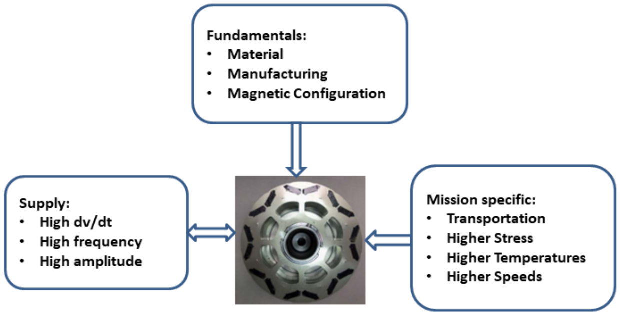

Fig.17. New considerations in designing electric machines.

must be able to withstand the operating requirements during the entire active lifetime of the electric machine. In industrial applications, a service life of 20,000 h is typically assumed. Over the past few decades, insulation systems for electrical machines have been dimensioned exclusively based on empirical values. If this practice is proved to be inadequate over the operating life, improvements are made as needed so that appropriate systems are developed over time. Three factors degrade the insulation and are described here: thermal stress, quality of the electrical supply, and mechanical load, all of which act on the winding's insulation system.

1) **Thermal stress**

In general, temperature is the most important parameter that determines the expected lifetime of a winding. Different insulation classes have different maximum allowed temperatures that the winding can be exposed to. Exceeding these values will degrade the insulative properties of the material and therefore shorten the lifetime of the winding. Following Montsinger's 8-degree rule from 1930 [54], the lifetime is expected to bisect with a temperature increase of 8 degrees.

Typically, safety tolerances are set very high, to avoid early machine failures, leading to overdesign of the system. However, in the context of electric propulsion systems, such an approach is no longer appropriate. Because of strict size and cost requirements on insulation systems, overdesigned approaches should be avoided. Currently, the focus is on the creation of cost-effective, compact, and lightweight insulation systems that can fulfill their function as an insulation medium during the entire service life of the machine. To meet these requirements, complex, earlier insulation system approaches (Figure 18) must be considered and transcended in the design process [55]. In recent years, electric propulsion motors with high filling factors (70% and higher) and high current densities (25 A/mm^2 and higher) have been designed and developed. These motors typically benefit from direct cooling to the end windings or through the installation of microchannels in the winding In these novel and somewhat complex cooling arrangements, proximity-induced thermal hot spots can appear that can jeopardize the health of the insulation. Likewise, exposure of the system permanent magnets to high temperatures can deteriorate their performance and eventually lead to irreversible demagnetization. Furthermore, in some driving scenarios, over time thermal cycling can put unprecedented fatigue on the winding insulation and lead to eventual failure.

2) **Electrical Stress**

Electric supply degradation due to electrical aging can occur during the operation of electrical machines depending on the applied voltage; therefore, this factor must be considered when designing the machine. Usually, a distinction is made between high-voltage machines (above 1,000 V) and low-voltage machines (below 1,000 V). For electrical machines with an operating voltage less than 1,000 V, the significance of electrical aging is low when operating at the main frequency (50/60 Hz) [55]. Such low voltages allow even thin layers of insulation to maintain the designed voltage. The sizing of the insulating materials is determined by the requirements for the mechanical strength of the winding.

However, electrical aging can become critical even below 1,000 V if the electrical machine is supplied by a power electronic inverter. In principle, voltage source inverters provide the electrical supply to the electrical machine in the form of pulse-width-modulated signals. Modulation of the voltage V with high switching frequencies and high dv/dt values results in voltage overshoots within a short time, which stresses the first few turns of the winding. This stress can lead to partial discharge even in the low -voltage range, causing permanent damage to the winding insulation system [56]. Therefore, for inverter-fed machines, especially those equipped with wide bandgap (WBG) switches, electrical stress due to the inverter must be considered when designing the insulation system. Furthermore, the presence of high-frequency current harmonics can cause proximity effects that alter the magnitude and distribution of losses within the windings. These can lead to thermal hot spots and create turn-turn short circuits. If these failures are not detected and treated, they can lead to catastrophic failure of the phase windings.

If the rated voltage is above 1,000 V, the thickness of the insulation layer must be determined from consideration of the voltage and the insulation strength of the material. High voltage can accelerate aging of the insulating material through partial electrical discharges that can stress the material. This can occur in cavities or air pockets in the material (known as void discharges) that results in local damage. If partial discharges occur over a long time, more and more material will erode to eventually cause a full breakdown of the insulation layer and associated total failure of the entire insulation system [55]. Notably, the tendency toward development of high-speed traction motors and gearboxes to achieve better power density usually requires operation at higher voltages (producing higher chances of partial discharge) and higher fundamental electrical frequency (producing higher rate of occurrence for partial discharge). which tend to penalize the longevity of the insulation. Furthermore, the higher rate of switching at high magnitudes of voltage will give rise to

This article has been accepted for publication in IEEE Transactions on Transportation Electrification. This is the author's version which has not been fully edited and content may change prior to final publication. Citation information: DOI 10.1109/TTE.2023.3321707

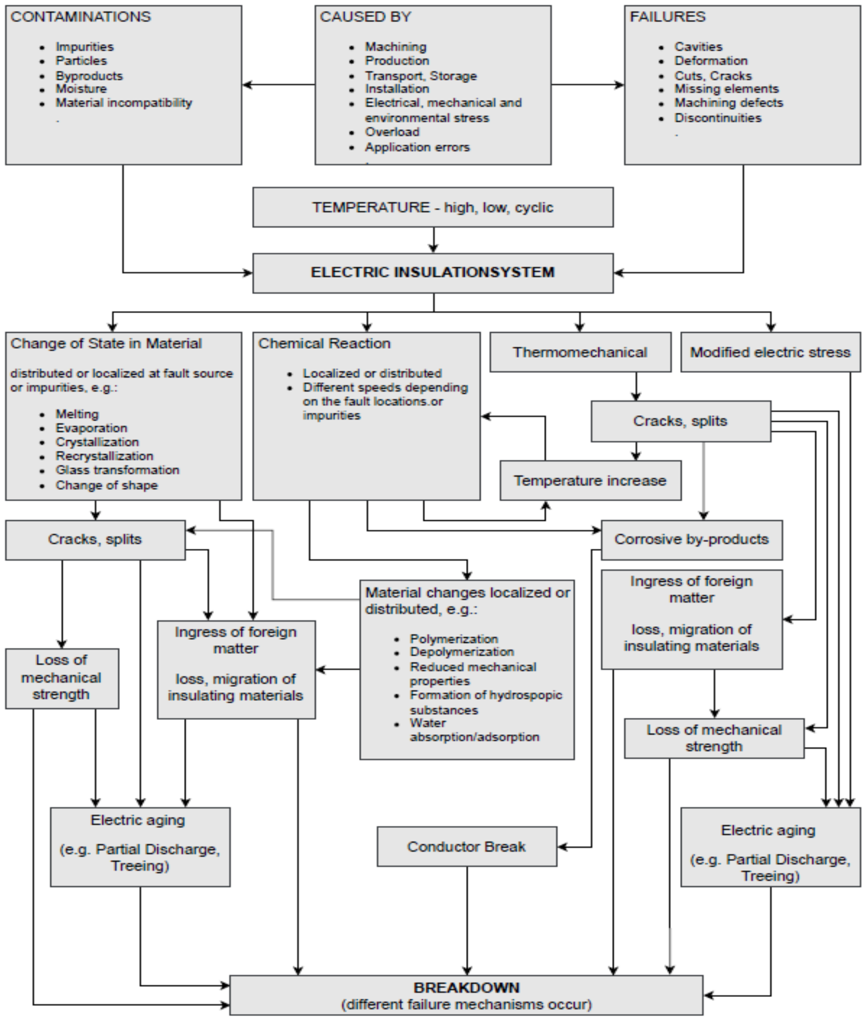

Fig. 18. Overview of the complex aging mechanisms in thermal aging (DIN EN 60505).

capacitive currents that are otherwise neglected in design. These capacitive paths can induce a significant voltage in the shaft, which may initiate arcing within the bearing system. The presence of capacitive currents through the insulation can also amplify the generation of heat, also leading to early failure of the insulation system.

When partial discharges occur in the material, the electrical aging can be described by means of the inverse power model, which mathematically describes an inverse power function. For the expected lifetime L of the insulation system, the correlation is obtained [57], [58].

3) Mechanical Issues

Mechanical aging originates from high mechanical stress on the insulating material. There are In the stator, two causes primarily lead to mechanical aging. The first cause is the vibrations generated by the operation of the electrical machine. Because of the rotary motion of the rotor, the vibrations resulting from minimal imbalances are transmitted to the stator via the bearings. There, the vibrations can cause the insulation system to vibrate. This type of mechanical stress is not dangerous for the winding insulation system. The contribution to mechanical aging is minimal and only becomes significant for high-speed drives. A more sever cause is stress due to the current flow in the two winding layers. The alternating current leads to a magnetic force oscillating at twice the power frequency, which is effective between the windings [59]. This force excites the windings to oscillate, causing the wire enamel layer of the Cu conductors to expand or compress. If the oscillations reach high amplitude, the deflection of the conductors also becomes large. These deflections cause the windings to oscillate, especially at points that are not firmly fixed, such as the winding head, which leads to abrasion of the surface of the insulating material due to friction with the metal sheet of the slot [56].

Transient processes in electrical machines also have similar effects that can occur during start-up or using power electronic inverters. The high current steepness due to the high switching frequencies can lead to short duration but high mechanical forces. The modeling of the effect of the mechanical load on the service life can be described by means of the inverse power model as in the case of electrical aging [58].

IV. Power Converter and Power Semiconductors

A. State of the Art

Tier 1 suppliers are offering ever-improving propulsion inverter solutions. However, many OEMs continue to develop their own propulsion inverter solutions in-house, which affords more flexibility with packaging and integration and supports rapid change while executing concurrent engineering with other vehicle teams. Battery voltages are still predominantly around 400 V, although an increasing number of production vehicles with 800–900 V buses are now in the market.

1) **Power semiconductor technology**

The choice of power semiconductor technology is a key decision in any inverter design. Over the past 30 years, Si IGBTs have predominantly been used in hybrid, battery, and fuel cell EVs. However, SiC MOSFETs are increasingly used and are expected to take over a growing market share through 2030. Supply is currently constraining the SiC market penetration, but increased capacity coming online over the next several years will help to relieve this bottleneck. Furthermore, SiC is more time-consuming and expensive to grow the raw material boule, and more challenging to split into discrete wafers. Wafer size is still predominantly 150 mm but will move into 200 mm fab in the near future.

Silicon carbide has been employed in both 400 and 800 V class systems. The main advantage of SiC is an increase in system efficiency, often by around 5%. Although SiC devices are still significantly more expensive than their equivalent Si counterparts, the added inverter cost is offset by either reduced battery cost for equivalent range or increased range for the same battery capacity. The basic SiC application-level design challenges have been largely addressed, and the remaining issues are supply chain, cost, and reliability.

IGBT devices, being unidirectional, require co-packaging of an anti-parallel diode. One key advantage of MOSFETs is the inherent body diode. Existing SiC inverters rely on the body diode to conduct during the brief dead-time and use the MOSFET channel to conduct the remainder of the reverse current flow. Eliminating the discrete anti-parallel diode provides more efficient use of space in the power device packaging area. Since MOSFETs conduct during the positive and negative half-cycles of the fundamental AC current waveform, at low motor speeds, the temperature pulsation at the die level is reduced compared with IGBT devices. This reduction can lead to less thermal cycling for SiC devices and help to minimize the fatigue mechanism. Furthermore, Si RC-IGBTs are on the market, which essentially combine the transistor and diode into one device on a single die. This makes for more efficient device packaging but may be better suited for drives with less regeneration and load on the diode.

Switching losses of SiC MOSFET devices can be significantly lower than those of IGBT devices. However, the actual benefits can be somewhat limited when considering factors such as voltage spike and dv/dt.

Voltage stress must be controlled at turn-on and turn-off events. A significant difference in SiC and Si is their diode reverse recovery characteristics. The Si PN diode has much larger reverse recovery current and slower recovery, whereas the SiC body diode is typically very fast. Voltage spike and ringing during SiC diode reverse recovery needs to be monitored over the full range of operating conditions, and the gate turn-on strength must be set accordingly. Creating a low-inductance DC link is critical to gaining the most benefit from the expensive SiC devices. High-performance, low–parasitic power modules are needed to get the best performance from these devices. The increased switching dv/dt can present EMC challenges, and a careful strategy is needed. The effects of dv/dt on motor insulation and bearing currents need to be included and addressed in the design trade-offs, as well. Although SiC inverters could be operated at higher switching frequencies, this does not necessarily offer dramatic size reduction as it would with a typical DC-DC converter because the motor size is not closely linked to switching frequency. The main component to benefit from increased switching frequency is the DC link X capacitor.

Notably, significant vehicle level efficiency improvement comes from the device conduction loss term. Although a propulsion inverter may need to be designed for a large, short duration peak load, the inverter current is on average quite small over a typical drive cycle. Comparing the forward voltage drop at peak current, a MOSFET implementation may have larger voltage drop compared with an IGBT device. However, for most of the current amplitudes during the drive cycle, the MOSFET will have lower forward drop because of the resistive nature of the channel.

2) **Device Packaging**

Device packaging approaches include discrete, half-bridge, and hex pack. The packaging could be single- or double-sided cooled using direct or indirect cooling. With direct cooling, a heat sink structure is attached directly to the power device as part of the baseplate structure. With indirect cooling, the interface to the heat sink is made via a thermal interface material. Some devices can be sintered to the heat sink, which offers a lower thermal impedance interface.

Two common module construction types are frame-based and transfer-molded. Frame-based types most often use silicone gel for dielectric sealing of the top side. Transfer-molded types encapsulate the internal structure within an epoxy molded body. Transfer molding is most often used on discrete or half-bridge modules. Signal pins can be solder or press fit types. Power connections are usually bolted joint or welded (resistance or laser weld). The choices typically depend on the manufacturing process capability available at the factory. Each inverter manufacturer must choose which approach aligns best with their packaging approach, manufacturing capability, production volume, and so on.

3) **Filtering**

Most production inverters employ both common mode and differential mode filtering at the DC interface. Differential filtering is limited to the large X capacitor. The DC link currents are too large to employ a discrete differential mode filter inductor. The cable inductance to the battery usually offers a small parasitic inductance, which helps keep the higher frequency harmonics within the inverter.

A DC link CM filter may include Y capacitors and a CM choke for a second-order filter. The CM choke is usually limited to one turn, such as bus bar pass through. Therefore, the core material must have the highest permeability, as well as good loss characteristics at the frequency range of interest. Nanocrystalline tape and ferrite are the primary choices. Impedance, temperature range, mechanical ruggedness, and cost are key parameters. As a result of the relatively small inductance value of the CM choke, the Y capacitors tend to be relatively large in value, between 0.1 and 1.0 µF per leg.

The X capacitors can take up a significant portion of the overall inverter volume. Maintaining a low inductance link to the power semiconductors is vital to obtaining the best performance. Most inverters utilize a large brick-style capacitor assembly, which is often custom-designed for optimal integration within the inverter unit. The capacitor usually includes multiple bobbins in parallel to achieve the desired capacitance and ripple current rating. The entire assembly is optimized to provide the lowest inductance. Thermal analysis and thermocouple testing are performed to ensure that the capacitor elements all remain within their acceptable operating limits in the expected stress profile.

Capacitor material has traditionally been metalized polypropylene films. Suppliers are continuously improving the film thickness and increasing the maximum temperature capability, although these improvements are incremental in nature. Some more recent developments involving thermoset type plastic films are showing promise and could result in more significant size reductions and higher-temperature operation of this component.

Placing the choke at the DC input does not prevent most currents from being generated between the inverter and the motor, but it does prevent those currents from flowing back onto the DC bus. Some inverters also place a CM filter at the AC interface to the motor. The advantage here is placing the choke element in series with the main parasitic path and directly reducing the amplitude of CM currents into the motor. This may reduce bearing currents and help with EMC.

4) **Sensing**

For AC current sensing, the Hall effect sensor with core is still the primary choice for hybrid, battery, and fuel cell EVs. However, various coreless Hall effect sensors have been increasingly used. Coreless sensors can offer reduced size, weight, and cost. When using coreless sensors, the effect of phase to phase cross-coupling and stray field should be carefully explored. These effects are sometimes mitigated with software-based decoupling of the sensed signals. Gain may be sensitive to mechanical alignments, so manufacturing tolerances are important. At least one OEM is still using resistive-based shunt.

Temperature sensing is often limited to the main power semiconductors and is usually accomplished with a thermistor placed on the power module substrate. However, the correlation of thermistor temperature can be complex, and predicting the junction temperature accurately for derating and protection purposes can be challenging. Another solution is to use on-die temperature sensing. A string of signal diodes is directly incorporated into the power semiconductor die structure. A small constant current is used to bias the diodes, and the forward voltage is measured. The known voltage versus temperature characteristic provides a means to accurately measure the junction temperature, which can provide reliable overtemperature protection under any operating conditions.

B. Future Trends

Silicon carbide devices have been used in EV traction drives since 2016 with the Tesla Model 3 [59]. In general, battery voltage and DC link voltage for EVs are increasing; 800 V is currently typical, and 1,000–1,200 V is estimated in the near future. Silicon carbide is the best candidate for higher-voltage applications; lateral and vertical GaN devices are also often considered for these voltage levels, but they are not yet mature enough to be used in traction inverters. Some lateral GaN devices can be used to build multilevel inverter-based traction drives, but these devices are mostly applicable to DC-DC converters used to power auxiliary systems, and they can also be used for onboard chargers. In an EV, multiple device technologies could coexist depending on the performance and cost.

Modern passenger EVs use a skateboard chassis with the battery in the body of the skateboard with the electric drives in the back, front, or both. To improve integration of the electric drive with the skateboard chassis, the electric drive needs a low profile and high volumetric power density. Because batteries are already quite heavy, by comparison, the weight of the electric drive is not a major concern. For an EV traction drive, the most important parameter is the cost, followed closely by volume and efficiency of the traction inverter and motor. DOE's Vehicle Technologies Office uses these three factors in its targets [61]. The 2025 targets for a 100 kW traction inverter include a $6/kW cost target and a 33 kW/L power density target, which is more than eight times higher than typical 2015 values.

WBG devices are attractive for EVs because of their low losses and high frequency operation, which result in more compact inverters and converters. Furthermore, they are required to achieve high–power density targets. Beyond 2030, all EVs will likely use WBG devices in their traction drives and the rest of the power conversion systems.

Power density: The power density target for the inverter is 100 kW/L, and the target for a traction motor is 50 kW/L. The three major components in an inverter that occupy most of the volume are the power module, heat sink, and DC link capacitor.

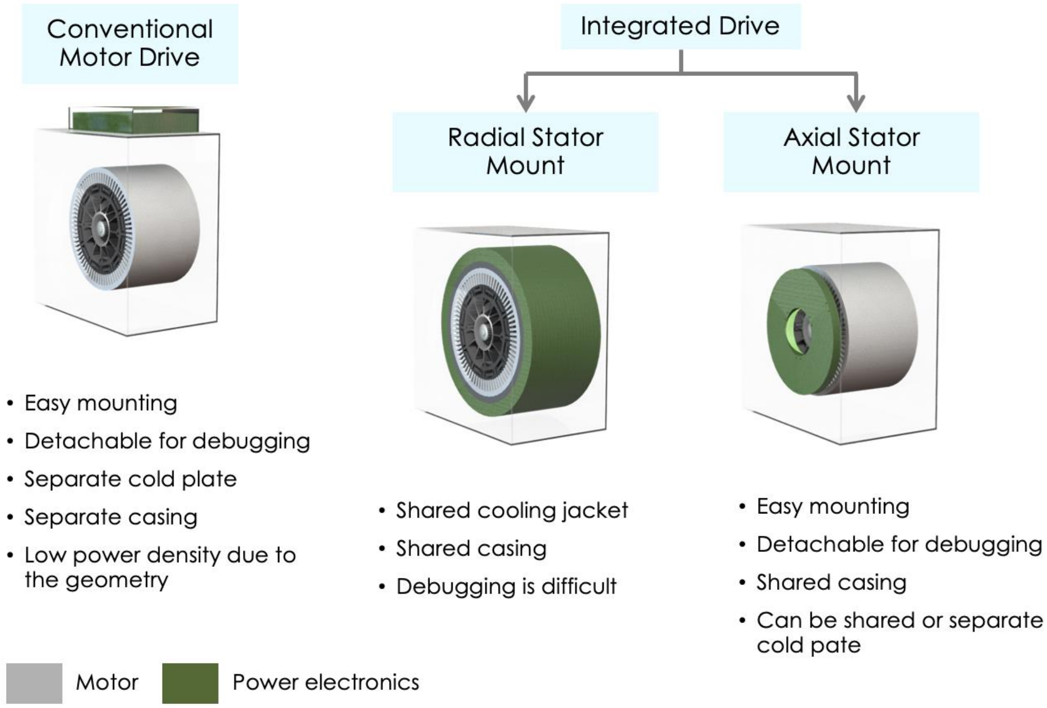

Fig. 19. Integrated drive system.

Power modules: WBG devices by themselves cannot achieve high power densities. Instead of stacking inverter components on top of each other, the components must be more closely integrated. A more integrated power module with an integrated gate driver, sensors, heat sinks, capacitors, and so on is needed. Double-sided packaging is preferred for better removal of heat from the power module at the expense of possible manufacturing complexity and yield issues. Integrating the gate driver and other electronics will require new multilayer substrates such as IMS [63] and organic DBC. By integrating the heat sink, the thermal interface material will be eliminated, thereby reducing thermal resistance in the thermal path.

Heat sinks: Lower losses of WBG devices reduce the stringent cooling requirements; however, smaller die areas also mean smaller surface areas for heat removal. Using technologies such as thermal pyrolytic graphite helps spread the heat to a wider area, and heat sink topology optimization technologies result in higher thermal conductivity. Reducing the size of heat sinks and reducing the thermal imbalance between the dies [63] increases reliability.

DC link capacitors: Film capacitors are used as DC link capacitors because of their self-healing mechanisms in case of failure; however, these capacitors take a substantial volume in the inverter because the link capacitor must pass up to 60% of the motor phase current. For a 2016 BMW i3, the DC link capacitor occupies a volume of 0.6 L. Considering the 2025 DOE Vehicle Technologies Office target of 1 L for a 100-kW inverter, the capacitor would occupy 60% of the total volume. Ceramic and PLZT capacitors are two alternatives not typically used as DC link capacitors in electric traction drives [60]. The ceramic capacitors fail short, which is undesirable for automotive manufacturers. PLZT capacitors are newer, and their failure mechanisms are not yet well understood. Since they have a polymer in addition to the ceramic as the dielectric, they might not fail short like their ceramic counterparts. Although the film capacitors are rolled into cylinders, some film capacitors suppliers have used a stacked approach similar to a deck of cards (e.g., EPCOS/TDK). Poly Charge Nano Lam caps also use stacked layers of material. The ceramic and PLZT capacitors are discrete components, and hundreds of them must be paralleled to achieve the capacitances needed for traction inverter DC links. Since these are small individual components, many of them can be embedded within the WBG-based power modules.

With WBG power devices coupled with new capacitor technologies, more integrated power modules, and optimized heat sinks, the 100 kW/L power density target can be achieved for a 100 kW and higher power rated traction inverters.

Integration of motor and converter: The phrase *integrated drives* in existing EVs typically refers to an inverter placed on top of a motor sharing a cooling system. Regarding the power electronics, an integrated drive would include the inverter inside or around the motor packaged together. Two options for integrated drives are an axial stator mount in which the inverter is placed by the end windings of the motor, and a radial stator mount in which the inverter is placed around the stator of the motor, as shown in Figure 19. Some research on integrated motors and inverters uses an H-bridge per motor coil, creating new opportunities for control. Another method that only works for outer rotor motors is to insert the inverter in the middle of the stator, which is now stationary in the middle of the motor (Figure 19). A hollow space can be designed where the inverter would be placed. This close connection would eliminate the need for long 3-phase cables to connect the inverter and the motor.

V. CONTROL

A. Drive Control

Control of electric current in an adjustable-speed motor drive system is essential in providing high performance. Whether for maximization of torque per Ampere, decoupling and ease of control, or mitigation of torque pulsation and acoustic noise, the control of electric current plays a crucial role. Since the design of electric machines is based on a symmetrical magnetic configuration, the supply to various phases needs to be symmetrical, as well. Furthermore, in the absence of a neutral point, the sum of the electric currents supplied to the machine must be zero. The sequence of excitation between phases determines the direction of rotating magnetic field and therefore the direction of motion.

Unlike internal combustion engines that exhibit their maximum torque at a particular speed, electric motors can provide their maximum torque at standstill and up to a speed at which the motional back-emf equals the available DC link voltage (i.e., the base speed). This unique capability provides an unparalleled advantage to electric motors in providing impressive startup acceleration, as observed in most EVs. To ensure maximum torque per Ampere operation, the excitation current needs to be in phase with the induced back-emf in each phase, and its waveform must follow that of the back-emf, albeit subject to thermal limitations of the machine and harmonic content of the back-emf. However, in IMs, exact implementation of this condition seems impossible because of the induction process. In the generating mode of operation, the phase current needs to be 180° out of phase with respect to the induced back-emf in the phase.

Equation (4) contains two components of torque: the reaction torque and the reluctance torque. The reluctance torque only exists if there is a magnetic saliency and qd-axis currents are not zero. Depending on the design of the machine, the balance between these terms may vary from no reluctance torque (i.e., induction motor) to no reaction torque (i.e., synchronous and switched reluctance machines). The IPMSM is a hybrid solution that benefits from both terms. In fact, the reluctance torque during startup process may be used to boost the accelerating torque.

Once the line-to-line induced voltage reaches the available DC link voltage, it is no longer possible to force the optimal current into the phase, and a phase advancing process is necessary. Introducing a phase shift between the phase current and induced back-emf allows for the current to reach its maximum value before facing the maximum back-emf. This process is known as field weakening, and in IPMSM drives, it is implemented by applying a negative current into the direct axis. Since the direct axis inductance is smaller than the quadrature axis current, the resulting reluctance torque will be positive and helps to extend the constant power region. Notably, the field weakening region will contribute to additional Cu and Si losses and is a key factor in sizing semiconductor devices. Furthermore, the PM-assisted synchronous reluctance motors in which magnets are installed in the quadrature axis do not benefit from the extended constant power speed ratio. In the absence of PMs (i.e., induction and reluctance machines), field weakening is implemented by reducing the positive direct axis current while maintaining the minimum required magnetization in the machine core. In MTPA control, the PF always lags, and torque can be controlled to the current limit of the inverter. During field weakening control, maximum power can be delivered, but the inverter voltage and current are limited. For PMSMs with characteristic current equal to maximum inverter current, power may be delivered under the maximum torque per volt, where the current trajectory leaves the current limit circle and moves parallel to the q-axis [62]. These operating modes demonstrate the close link between machine and controller designs.

Figure 20 shows how an electric machine can operate as a motor or generator in both directions of rotation. On the axes, the two main parameters required for the electric machine performance are torque and speed. Figure 21 illustrates an example of the control system for a speed-controlled 2-pole PMSM in the constant torque region (i.e., $e^{-j\theta_r}$ denotes the Park transformation) In the field weakening region, the reference value for the direct axis current will be a negative figure that is adequately adjusted as a function of the operating speed.

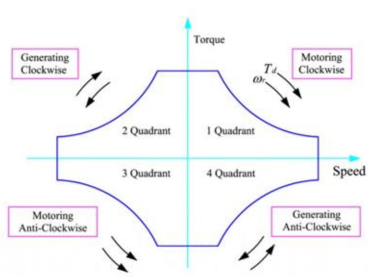

Fig. 20. Electric machine operation.

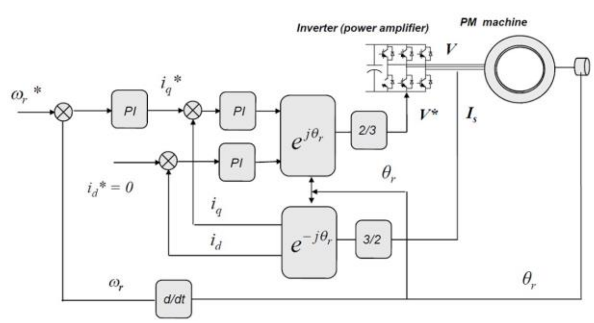

Fig. 21. Example electric drive system.

B. Position sensorless control

Rotor position is critical to properly synchronize the stator current with the back-emf of the phase. Hall effect sensors, optical encoders, and resolvers are typically used to explicitly obtain the rotor position. However, integration of position sensors increases the vulnerability of the control systems to additional failures, so position sensorless control as a backup system or to reduce the cost and size of the drive system are necessary. The induced back-emf in induction- and surface-mounted PM motor drives provides the necessary means to synchronize the stator currents. However, detection of back-emf at very low speeds is subject to inaccuracy and numerical challenges. This continues to be an active area of research. In electric machines with a reluctance torque component, the working inductances of the machine vary with the rotor position, and the encoded position information can be used to synchronize the stator current, which is another benefit of IPMSMs.

C. Mitigation of acoustic noise and vibration

NVH is an important figure of merit for electric propulsion systems. The reluctance component of torque introduces torque pulsation due to its dependence on rotor position. Furthermore, the change in reluctance between PMs and stator slots generates an oscillating component of torque (i.e., cogging torque). These pulsations will trigger tangential vibration on the stator frame that leads to acoustic noise. In addition, the presence of substantial radial forces acting on the stator frame, especially in switched reluctance machines, introduces severe radial vibration of the stator. These vibrations will be transmitted to the outer race of the bearing and can excite additional vibration and noise in the endcap and bearings. Among various electric machines, induction motors provide the least magnitude of pulsation and acoustic noise. In other types of electric machines, adequate design and current shaping algorithms are necessary to mitigate undesirable acoustic noise and vibration. However, these techniques tend to penalize the average torque of the motor.

D. Connectivity and intelligence

Connectivity and communication are crucial in electric propulsion systems. The ability for remote monitoring and remote updating in the control algorithm will provide the much-needed resilience and safety of the powertrain. Continuous health monitoring of electric drive systems and timely maintenance of inverters and motors will introduce new layers of fault tolerance. Furthermore, use of artificial intelligence for health monitoring of motors and converters, self-tuning of controls, and detection of remaining useful lifetime in system components is expected to become prevalent in the future.

E. Future trends

Access to fast controllers and communication opens new horizons in integration of additional parameters such as road profile, historical driving habits, and ambient conditions in the system level control of electric propulsion systems. For instance, thermal management of the motor drive system with real time expectation will provide ample opportunities for improving fault tolerance and durability of the propulsion system. Use of artificial intelligence for approximate reasoning under complex driving scenarios will further improve the overall performance of the system. Adaptive control in the presence of parameter variation caused by ageing and fatigue are among other future characteristics of the controller that can provide the best performance given the condition of the electric propulsion system.

VI. Functional Safety

Although modern electric propulsion systems have several advantages, their dependence on complex subsystems, including electric machines, drive systems, and batteries, can increase the risk of system faults [65]. To avoid or mitigate such risks, a high level of dependability is required [66].

Functional safely is an important aspect of dependability for electric drive vehicles and should be addressed throughout their development cycle [66]–[68]. ISO 26262 is the standard for functional safety of electrical and electronic systems within a car during different development process phases [67]. By following this standard and using risk analysis methods such as failure modes and effects analysis, the potential hazards resulting from failure of electrical or electronics components, as well as their causes and effects, can be identified and evaluated systemically. ISO 26262 also suggests a clear guidance for manufacturers to achieve required Automotive Safety Integrity Level employing different approaches such as driving warning, redundant systems, and fault detection, isolation, and reconfiguration (FDIR) algorithms [68], [71].

Electric machines, drive systems, and batteries are vulnerable to different types of faults. Tables II and III list the most common faults in electric machines and drive systems [72]–[76].

To avoid the described failures, various fault tolerance techniques have been developed or are under investigation. Fault detection and isolation is a common solution to address such faults. In this technique, some health indicators of the system are checked to detect, locate, and isolate faults [63], [67], [73]. An example of fault detection and isolation implementation in electric drive vehicles is for detecting and isolating current sensor faults, where the inverter and motor go to a zero-torque output safe mode.

FDIR is an alternative solution when a higher level of safety integrity is required. In this method, full or partial functional recovery can be achieved using redundant or alternative components. A dual inverter–fed open-end winding machine is an implementation of FDIR methods for power switch faults. In such a system, once the open circuit fault occurs in one switch, the motor continues its operation in a 2-phase mode. However, in the 2-phase fault tolerant operation mode, each phase current is higher than machine phase currents in the normal 3-phase mode, and thus, 2-phase torque is lower than the torque in the 3-phase mode [77]–[79]. Power leg sharing and adding one additional power leg to the inverter are also alternatives to address power switches faults [79], [80]. In FDIR methods, virtual redundancy can be used to improve reliability against sensor faults; the faulty sensor data can be virtually determined using machine modeling and the data received from other sensors [81]. Table IV lists the most common faults in Li^+ EVs battery packs [62], [82]– [84]. The battery pack failures can be caused by faults in the battery management system or in cells.

The battery management system is critical for safe operation of batteries, and its malfunction can lead to battery overcharge, excessive discharge of cells, or cell imbalance, possibly leading to battery damage and fire. SAE International standard J2990 describes procedures to be used by first (police and fire department) and second (EMT) responders when addressing hybrid, battery, and fuel cell EV crashes. The estimation accuracy of a battery state of charge and state of health in a battery management system is highly dependent on the accuracy of hundreds of sensors installed in the battery pack

TABLE II
FAULTS IN ELECTRIC MACHINES [72]–[76]

Type	Physical part	Fault mode	Failure
Electrical	Stator	Phase short circuit	Demagnetization, large disturbance torques
		Phase open circuit	High torque ripple, loss of torque
		Interturn short circuit	Vibration, harmonics, reduced performance, insulation failure
	Rotor	PMSM: Demagnetization	Reduced efficiency, reduced torque
		IM: Broken bar	Increased NVH, increased torque ripple, overheating
Thermal	Rotor/stator/end winding	Motor cooling system fault	Motor overtemperature, derating
		Extreme ambient temperatures	
Mechanical	Bearing	Rolling element bearing defects	Increased NVH, reduced efficiency, reduced lifetime of machine
	Assembly	Airgap eccentricities (static and dynamic)	Increased NVH, rotor-stator contact, faster bearing wear, reduced torque, reduced efficiency
Sensor	Rotor/stator	Temperature sensor fault	Motor overtemperature
		Rotor angle fault	Disturbance torques, reverse voltage leads to demagnetization

TABLE III
FAULTS IN ELECTRIC DRIVES [72]– [74]

Type	Physical part	Fault mode	Failure
Electrical	Power switches	Short circuit fault	Excess current, sever damage to power switches, large disturbance torques
		Open circuit fault	Significant torque pulsations, reduced torque, reduced efficiency, increased heat
	Capacitor	Short circuit fault	Excess current on battery, large disturbance torques
		Open circuit fault	High voltage ripple, increased torque ripple, accelerated power switches failure
		Degradation	Increased equivalent series resistance leading to increased heat
Thermal	Power switches	Inverter cooling system fault	Power switches overheating and damage, derating
		Extreme ambient temperatures	
Sensor	Power switches/control bord/DC bus	Current sensors	Overcurrent of power switches and stator, wrong estimation of torque leading to unwanted torque
		DC bus voltage sensors	Wrong estimation of inverter output voltage leading to unwanted torque, motor overheating, demagnetization

TABLE IV
FAULTS IN Li^+ BATTERIES [72], [82]–[84]

Type	Physical part	Fault mode	Failure
Electrical	Battery management system	Hardware faults	Overcharge, battery damage
			Excessive discharge, deep discharging, battery damage
			Cell imbalance, battery damage
	Cells	Increased internal resistance	Reduced voltage, overheating, increased loss
		Short circuit	Thermal runaway, fire hazard
Mechanical	Cells	Electrolyte leakage	Environmental impact, contact with human skin and eyes, short circuit in adjacent electrical and electronic systems
Thermal		Battery cooling system faults	Overheating, cell thermal runaway
		Extreme ambient temperatures	
		Thermal runaway	Damaged beyond repair to battery, fire hazard, explosion
Sensor	Battery management system/cells	Voltage sensors	Incorrect estimation of state of charge and state of health, running outside the safe operating area of the battery, cell overheating, fire hazard

to measure current, voltage, and temperature of each cell, and any fault in battery pack sensors can cause the battery to run outside its safe operating area. Therefore, to avoid failures such as cell thermal runaway, detection and isolation of sensors faults are required [72], [82]–[84]. Furthermore, because the battery short circuit can lead to thermal runaway and explosion, early detection and isolation of such faults is vital [83]. The validity of fault detection and isolation and FDIR methods developed to address the faults in battery cells and battery sensors highly relies on the accuracy of battery models, so accurate battery modeling is required [82]–[85].

VII. COMMERCIALLY AVAILABLE AUTOMOTIVE PROPULSION SYSTEMS

Interior permanent magnet synchronous machines dominate the automotive electric propulsion motors. With a few exceptions where induction and PM-assist synchronous motors have been used in mild hybrid and other commercial vehicles, most propulsion motors use IPMSM configuration that use rare earth metals and is powered using a three-legged power electronic inverter. Although an apples-to-apples comparison of the power density and specific power of these machines may not provide the full picture of their performances, high running efficiency and exceptional specific power has been common among this family of electric drives. Use of transmission has played a key role in increasing the specific power of the motors. Similarly, use of wide bandgap SiC devices allows for higher switching frequency so that the inverter becomes smaller. Volatile cost of RE sintered magnets, concerns regarding the impact of demagnetization, sustained short circuit on fault tolerant operation, safety, limited high speed performance caused by high back-emf, and durability in IPMSM has convinced some manufacturers to investigate alternates such as wound rotor synchronous machines with wireless transfer of excitation current into the rotor. Research and development on other configurations with reduced or no use of RE in industry continues and in recent years SRM, axially laminated synchronous reluctance motor, and induction motor have been targeted for off-road vehicle, passenger cars, and locomotion respectively. Table V summarizes a comparison among commercially available automotive electric propulsion systems in terms of their power densities [85]. It is notable that many of these systems meet or exceed the requirements of the DoE by a tangible margin. Furthermore, specific operating parameters for the listed electric propulsion systems have been reported by the Oak Ridge national laboratory in the same report [86] (See Table VI). Finally, the new targets of DoE for 2025 mandates 50% reduction in cost ($/kW), 843% increase in power density (kW/L), 100% increase in power level, and 100% increase in reliability/lifetime [87].

TABLE V

COMPARISON OF ELECTRIC PROPULSION SYSTEMS IN COMMERCIAL VEHICLES [83]

Parameter	**2022 DoE Goal (55kW)**	**2004 Prius (50kW)**	**2007 Camry (70kW)**	**2008 Lexus (LS600h) (110kW)**	**2010 Prius (60kW)**	**2011 Sonata (30kW)**	**2012 Leaf (80kW)**	**2014 Honda Accord (124kW)**	**2016 BMW i3 (125kW)**	**2017 Prius (53kW)**
Motor										
Peak Power Density(kW/L)	**5.7**	3.3	5.9✓	6.6✓	4.8	3	4.2	8.5✓	9.1✓	5.7✓
Peak specific power (kW/kg)	**1.6**	1.1	1.7✓	2.5✓	1.6	1.1	1.4	2.9✓	3✓	1.7✓
Inverter Excludes generator inverter and parenthetical values exclude boost converter mass and volume)										
Peak Power Density (kW/L)	**13.4**	4.5(7.4)	7.4(11.7)	10.6(17.2) ✓	5.9(11.1)	7.3	5.7	12.1(18.5) ✓	18.5✓	11.5(21.7) ✓
Peak specific power (kW/kg)	**14.1**	3.8(6.2)	5 (9.3)	7.7(14.9) ✓	6.9(16.7)	6.9	4.9	9.1 (21.7) ✓	14.1✓	8.6 (19) ✓

TABLE VI

COMPARISON OF DEVICE AREA

Parameter	**2004 Prius (50kW)**	**2007 Camry (70kW)**	**2008 Lexus (LS600h) (110kW)**	**2010 Prius (60kW)**	**2011 Sonata (30kW)**	**2012 Leaf (80kW)**	**2014 Honda Accord (124kW)**	**2016 BMW i3 (125kW)**	**2017 Prius (53kW)**
DC Voltage	500	650	650	650	270	375	700	355	600
Current(A-rms)	225	282	304	170	212	442	300	375	
IGBT die Area (mm^2)	131.9	120.3	163.3	109.4	99.2	225	185.3	99.3	159.7
Number of IGBTs	12	18	12	12	12	18	12	24	6
IGBT total Silicon Area	1582.8	1689.6	1969.6	1312.8	1189.8	4050	2223.12	2382.96	958.1
Motor power/total area	34.75	48.49	81.65	45.7	25.21	19.75	55.78	52.46	55.32

VIII. Conclusions

This article examines the state-of-the-art and future trends in design and development of electric propulsion systems. Better usage of material, improvement in efficiency, cost, fault tolerance, and size are primary focuses of the research community. A rather fast-growing market for electrified transportation may supersede successful development and integration of technologies that optimize these focuses, but a sustainable, affordable, and environmentally friendly automotive industry must address these outstanding challenges. The successful realization of this paradigm shift will bring profound changes in global energy generation, transmission, and consumption with unparalleled flexibility and opportunities. The environmental, geopolitical, and financial effects of this transformation are immeasurable. It is expected that the choice of motor to become more diverse and reduced-RE and non-RE configurations will become more prevalent in coming years. Wound rotor synchronous machines, induction and reluctance machines can justifiably find their rightful place among propulsion motors. Concerns regarding sustainability, fault tolerance, and cost are the main drivers in this transition from a dominant RE-based IPMSM industry. Use of wide bandgap devices, more compact packaging, and integration of compact passive elements with DC-link and power modules tend to further increase the power density of power converters and their thermal/physical integration with the propulsion motors will offer substantial reduction in overall, size, cost, and modularity of the drive systems. Recycling of raw material and components and use of new manufacturing techniques such as 3-D printing will offer new opportunities that may allow for a less costly manufacturing and disassembly of electric motors and power converters, thereby reducing cost and enhancing the sustainability of the entire process.

References

[1] Global Electric Vehicle Market 2023-2027, Infiniti Research Limited, 2023.

[2] E. Gurpinar and B. Ozpineci, "Loss Analysis and Mapping of a SiC MOSFET Based Segmented Two-Level Three-Phase Inverter for EV Traction Systems," *2018 IEEE Transportation Electrification Conference and Expo*, 1046–1053, 2018.

[3] M. Ehsani, K. V. Singh, H. O. Bansal, and R. T. Mehrjardi, "State of the art and trends in electric and hybrid electric vehicles," *Proceedings of the IEEE* 109(6), 967–984, 2021.

[4] A. Dik, S. Omer, and R. Boukhanouf, "Electric Vehicles: V2G for Rapid, Safe, and Green EV Penetration," *Energies* 15(3), 803, 2022.

[5] J. M. D. Coey, *Magnetism and Magnetic Materials*, Cambridge University Press, 2010.

[6] https://www.edmunds.com/car-news/auto-industry/2017-tesla-model-3-has-unexpected-electric-motor-design.html

[7] L. H. Lewis and F. Jiménez-Villacorta, "Perspectives on permanent magnetic materials for energy conversion and power generation," *Metallurgical and Materials Transactions A* 44(1), 2–20, 2013.

[8] R. W. McCallum, L. H. Lewis, R. Skomski, M. J. Kramer, and I. E. Anderson, "Practical aspects of modern and future permanent magnets," *Annual Review of Materials Research* 44, 451–477, 2014.

[9] D. Egorov, I. Petrov, J. J. Pyrhönen, J. Link, R. Stern, P. Sergeant, and B. Sarlioglu, "Hysteresis Loss in NdFeB Permanent Magnets in a Permanent Magnet Synchronous Machine," *IEEE Transactions on Industrial Electronics* 69(1), 121–129, 2022.

[10] K. Bourzac, "The rare-earth crisis," *Technology Review* 114(3), 58–63, 2011.

[11] B. J. Smith and R. G. Eggert, "Multifaceted material substitution: The case of NdFeB magnets, 2010–2015," *Journal of Metals* 68(7), 1964–1971, 2016.

[12] Reuters Staff, "New Toyota magnet cuts dependence on key rare earth metal for EV motors," Reuters, February 20, 2018. [Online] Available at https://www.reuters.com/article/us-toyota-magnet/new-toyota-magnet-cuts-dependence-on-key-rare-earth-metal-for-ev-motors-idUSKCN1G413F.

[13] "Executive Order on Addressing the Threat to the Domestic Supply Chain from Reliance on Critical Minerals from Foreign Adversaries," D. J. Trump, The White House, September 30, 2020; "Executive Order on America's Supply Chains," J. R. Biden, The White House, February 24, 2021; "President Biden's Bipartisan Infrastructure Law," J. R. Biden, The White House, August 2022.

[14] J. M. D. Coey, "Permanent magnets: Plugging the gap," *Scripta Materialia* 67(6), 524–529, 2012.

[15] K. P. Skokov and O. Gutfleisch, "Heavy rare earth free, free rare earth and rare earth free magnets-Vision and reality." *Scripta Materialia* 154, 289–294, 2018.

[16] J. Cui, M. Kramer, L. Zhou, F. Liu, A. Gabay, G. Hadjipanayis, B. Balasubramanian, and D. Sellmyer, "Current progress and future challenges in rare-earth-free permanent magnets," *Acta Materialia* 158, 118–137, 2018.

[17] L. H. Lewis, et al., "Inspired by nature: investigating tetrataenite for permanent magnet applications," *Journal of Physics: Condensed Matter* 26(6), 064213, 2014.

[18] R. Brand, "Beyond Electrical Steel," *Magnetics Technology International* 62–65, 2014.

[19] G. Herzer, "Modern soft magnets: Amorphous and nanocrystalline materials," *Acta Materialia* 61(3), 718–734, 2013.

[20] G. K.-J. G. Betz, "Visualisation of magnetic domain structures and magnetisation processes in Goss-oriented, high permeability steels using neutron grating interferometry," *École Polytechnique Fédérale de Lausanne Pour L'Obtention du Grade de Docteur Ès Sciences* 7002, 2016.

[21] "Electrical steel: The heart of an electric motor," Thyssenkrupp. [Online] Available at https://www.thyssenkrupp.com/en/company/innovation/sustainable-mobility/electrical-steel.html.

[22] J. M. Silveyra, E. Ferrara, D. L. Huber, and T. C. Monson, "Soft magnetic materials for a sustainable and electrified world," *Science* 362(6413), eaao0195, 2018.

[23] A. Adib, et al., "E-Mobility — Advancements and challenges," *IEEE Access* 7, 165226–165240, 2019.

[24] R. Mehrabian, "Rapid solidification," *International Metals Reviews* 27(1), 185–208, 1982.

[25] Y. Yoshizawa, S. Oguma, and K. Yamauchi, "New Fe-based soft magnetic alloys composed of ultrafine grain structure," *Journal of Applied Physics* 64(10), 6044–6046, 1988.

[26] G. Herzer, "Modern soft magnets: Amorphous and nanocrystalline materials," *Acta Materialia* 61(3), 718–734, 2013.

[27] B. T. Lejeune, R. Barua, E. Simsek, R. W. McCallum, R. T. Ott, M. J. Kramer, and L. H. Lewis, "Towards additive manufacturing of magnetocaloric working materials," *Materialia* 16, 101071, 2021.

[28] T. N. Lamichhane, L. Sethuraman, A. Dalagan, H. Wang, J. Keller, and M. P. Paranthaman, "Additive manufacturing of soft magnets for electrical machines—A review," *Materials Today Physics* 15, 100255, 2020.

[29] K. Li, J. Z. Bird, and V. M. Acharya, "Ideal Radial Permanent Magnet Coupling Torque Density Analysis," *IEEE Transactions on Magnetics* 53(6), 2017.

[30] K. K. Uppalapati, W. Bomela, J. Z. Bird, M. Calvin, and J. Wright, "Construction of a Low Speed Flux Focusing Magnetic Gear," *2013 IEEE Energy Conversion Conference and Exposition*, Denver, Colorado, September 15–19, 2013.

[31] H. Y. Wong, H. Baninajar, B. Dechant, and J. Bird, "Designing a Magnetic Gear for an Electric Aircraft Drivetrain," *2020 IEEE Energy*

Conversion Conference and Exposition, Detroit, Michigan, October 11–15, 2020.

[32] S. Sirimanna, T. Balachandran, N. Salk, J. Xiao, D. Lee, and K. Haran, "Electric Propulsors for Zero-Emission Aircraft Partially Superconducting Machines," *IEEE Electrification Magazine* 10(2), 43–52, 2022.

[33] J. Ley and J. Lutz, "FreedomCAR Advanced Traction Drive Motor Development Phase I," ORNL/TM-2006/UQM, Oak Ridge National Laboratory, 2006.

[34] J. M. Bailey and J. W. McKeever, "Fractional-Slot Surface Mounted PM Motors with Concentrated Windings for HEV Traction Drives," ORNL/TM-2005/183, Oak Ridge National Laboratory, 2005.

[35] J. Wang, W. Geng, Q. Li, L. Li, and Z. Zhang, "A New Flux-Concentrating Rotor of Permanent Magnet Motor for Electric Vehicle Application," *IEEE Transactions on Industrial Electronics* 69(11), 10882–10892, 2022.

[36] N. Dave, X. Zhang, Z. Xu, D. Grada, H. Zhang, J. Li, G. Vakil, C. Gerad,"Carbon emission comparison of slotted and slottless motors for eVTOL application", *Proceeding of 2022 IEEE/AIAA Transportation Electrification Conference and Electric Aircraft Symposium*, pp. 1291-1295, July 2022, Anaheim, CA, USA.

[37] W. Bomela, J. Z. Bird, and V. M. Acharya, "The Performance of a Transverse Flux Magnetic Gear," *IEEE Transactions on Magnetics* 50(1), 2014.

[38] Ayman El-Refaie *et. al.*, "Comparison of traction motors that reduce or eliminate rare-earth materials," *IET Electrical Systems in Transportation*, 2017, Volume 7, Issue 3, pp. 207-214.

[39] M. Abbasian, B. Fahimi, and M. Moallem, "High Torque Double–Stator Switched Reluctance Machine for Electric Vehicle Propulsion," *2010 IEEE Power and Propulsion Conference*, Lille, France, September 1–3, 2010.

[40] A. Credo, G. Fabri, M. Villani, and M. Popescu, "Adopting the topology optimization on the design of high – speed synchronous reluctance motors for electric vehicles," *IEEE Transactions on Industry Applications* 56(5), 5429–5438, 2020.

[41] G. Berardi, S. Nategh, N. Bianchi, Y. Thioliere," A comparison between random and hairpin winding in E-mobility applications", *Proceedings of IEEE Industrial Electronics Society Annual Conference* (IECON) 2020, November 2020, Singapore, pp. 815-820.

[42] I. Boldea, A. A. Popa, and L. Tutelea, "Optimal design of variable speed electric motor-generator drives: An overview," *Proceedings of the Romanian Academy Series A: Mathematics Physics Technical Sciences Information Science* 23(2), 171–185, 2022.

[43] T. Orosz, et al., "Robust design optimization and emerging technologies for electrical machines: Challenges and open problems," *Applied Sciences* 10(19), 6653, 2020.

[44] Q. Ma, et al., "A Review of Electrical Machine Optimization Methods with Emphasis on Computational Time," *2019 IEEE International Electric Machines & Drives Conference*, 2019.

[45] S. D. Sudhoff, Power Magnetic Devices: A Multi-Objective Design Approach, John Wiley & Sons, 2021.

[46] M. Bash, S. Pekarek, S. Sudhoff, J. Whitmore, and M. Frantzen, "A comparison of permanent magnet and wound rotor synchronous machines for portable power generation," *2010 Power and Energy Conference at Illinois*, Urbana, Illinois, 1–6, 2010.

[47] T. Song, et al., "Multi-physics and multi-objective multiphysics design of interior permanent magnet synchronous motor for electric vehicles," *IET Electric Power Applications* 14(11), 2243–2254, 2020.

[48] X. Sun, et al., "Multiobjective and multiphysics design optimization of a switched reluctance motor for electric vehicle applications," *IEEE Transactions on Energy Conversion* 36(4), 3294–3304, 2021.

[49] "Aviation-Class Synergistically Cooled Electric-Motors with Integrated Drives (ASCEND)," DE-FOA-0002238, *US Department of Energy*, 2019.

[50] Y. Gao, V. Sankaranarayanan, E. M. Dede, A. Ghosh, D. Maksimovic, and R. W. Erickson, "Drive-Cycle Optimized 99% Efficient SiC Boost Converter Using Planar Inductor with Enhanced Thermal Management," *2019 20th Workshop on Control and Modeling for Power Electronics*, Toronto, Canada, 1–7, 2019.

[51] T. J. Miller, "SPEED's Electric Motors," *University of Glasgow*, 2002.

[52] "Electrical and Electronics Technical Team Roadmap," U. S. DRIVE, US Department of Energy, 2019. [Online] Available at https://www.energy.gov/eere/vehicles/articles/us-drive-electrical-and-electronics-technical-team-roadmap.

[53] Energy Trends in Selected Manufacturing Sectors: Opportunities and Challenges for Environmentally Preferable Energy Outcomes, US Environmental Protection Agency, 2007.

[54] V. M. Montsinger, "Loading Transformers by Temperature," *Transactions of the American Institute of Electrical Engineers* 49(2), 776–790, 1930.

[55] G. C. Stone, I. Culbert, E. A. Boulter, and H. Dhirani, *Electrical Insulation for Rotating Machines*, John Wiley & Sons, 2014.

[56] M. Kaufhold, K. Schäfer, K. Bauer, A. Bethge, J. Risse, "Interface phenomena in stator winding insulation – challenges in design, diagnosis, and service experience," *IEEE Electrical Insulation Magazine* 18(2), 27–36, 2002.

[57] R. A. Morin and R. Bartnikas, "Multistress Aging of Stator Bars in a Three-Phase Model Stator Under Load Cycling Conditions," *IEEE Transactions on Energy Conversion* 27(2), 374–381, 2012.

[58] G. Mazzanti, G. C. Montanari, L. Simoni, and M. B. Srinivas, "Combined electro-thermo-mechanical model for life prediction of electrical insulating materials," *Conference on Electrical Insulation and Dielectric Phenomena, 1995*, 274–277, 1995.

[59] M. Ohtaguro, K. Yagiuchi, and H. Yamaguchi, "Mechanical Behavior of Stator Endwindings," *IEEE Transactions on Power Apparatus and Systems* PAS-99(3), 1181–1185, 1980.

[60] Y. Yang, L. Dorn-Gomba, R. Rodriguez, C. Mak, and A. Emadi, "Automotive Power Module Packaging: Current Status and Future Trends," *IEEE Access* 8, 160126–160144, 2020.

[61] Electrical and Electronics Technical Team Roadmap, U. S. DRIVE, US Department of Energy, 2017.

[62] S. Chowdhury, E. Gurpinar, and B. Ozpineci, "Capacitor Technologies: Characterization, Selection, and Packaging for Next-Generation Power Electronics Applications," *IEEE Transactions on Transportation Electrification* 8(2), 2710–2720, 2022.

[63] S. Chowdhury, E. Gurpinar, and B. Ozpineci, "Characterization and Analysis of Insulated Metal Substrate-Based SiC Power Module for Traction Application," *2020 IEEE Energy Conversion Congress and Exposition*, 195–202, 2020.

[64] S.-K. Sul, *Control of Electric Machine Drive Systems*, IEEE Press, John Wiley & Sons, Inc., 2011.

[65] R. Sahu, E. Gurpinar, and B. Ozpineci, "Liquid-Cooled Heat Sink Optimization for Thermal Imbalance Mitigation in Wide-Bandgap Power Modules," *Proceedings of the ASME 2020 International Technical Conference and Exhibition on Packaging and Integration of Electronic and Photonic Microsystems* V001T07A001, October 27–29, 2020.

[66] L. Zhang, et al., "Fault-tolerant control for intelligent electrified vehicles against front wheel steering angle sensor faults during trajectory tracking," *IEEE Access* 9, 65174–65186, 2021.

[67] A. Avizienis, et al., "Basic concepts and taxonomy of dependable and secure computing," *IEEE Transactions on Dependable and Secure Computing* 1(1), 11–33, 2004.

[68] J. Zhang, H. Yao, and G. Rizzoni, "Fault diagnosis for electric drive systems of electrified vehicles based on structural analysis," *IEEE Transactions on Vehicular Technology* 66(2), 1027–1039, 2016.

[69] C. Becker, A. Nasser, and F. Attioui, Functional Safety Assessment of a Generic Accelerator Control System With Electronic Throttle Control in Fuel Cell Hybrid Electric Vehicles, DOT HS 812 640, US Department of Transportation, National Highway Traffic Safety Administration, 2018.

[70] A. Avizienis, et al., "Basic concepts and taxonomy of dependable and secure computing," *IEEE Transactions on Dependable and Secure Computing* 1(1), 11–33, 2004.

[71] C. Becker, A. Nasser, and F. Attioui, Functional Safety Assessment of a Generic Accelerator Control System With Electronic Throttle Control in Fuel Cell Hybrid Electric Vehicles, DOT HS 812 640, US Department of Transportation, National Highway Traffic Safety Administration, 2018.

[72] N. H. Obeid, et al., "Early intermittent interturn fault detection and localization for a permanent magnet synchronous motor of electrical vehicles using wavelet transform," *IEEE Transactions on Transportation Electrification* 3(3), 694–702, 2017.

[73] A. Cordoba-Arenas, J. Zhang, and G. Rizzoni, "Diagnostics and prognostics needs and requirements for electrified vehicles powertrains," *IFAC Proceedings Volumes* 46(21), 524–529, 2013.

[74] J. Zhang, et al., "An integrated fault isolation and prognosis method for electric drive systems of battery electric vehicles," *IEEE Transactions on Transportation Electrification* 7(1), 317–328, 2020.

[75] K. Lee and M. Lee, "Fault-tolerant stability control for independent four-wheel drive electric vehicle under actuator fault conditions," *IEEE Access* 8, 91368–91378, 2020.

[76] Y. Qi, et al., "Analysis and detection of inter-turn short-circuit fault through extended self-commissioning," *IEEE Transactions on Industry Applications* 53(3), 2730–2739, 2016.

[77] S. S. Nair, V. I. Patel, and J. Wang, "Post-demagnetization performance assessment for interior permanent magnet AC machines," *IEEE Transactions on Magnetics* 52(4), 1–10, 2015.

[78] U. R. Muduli, et al., "Interrupt-free operation of dual-motor four-wheel drive electric vehicle under inverter failure," *IEEE Transactions on Transportation Electrification* 7(1), 329–338, 2020.

[79] A. Ghaderi, "Motor control method, power conversion device, motor module, and electric power steering device," Patent No. US 11,190,124 B2, November 30, 2021.

[80] Y. Zuo, et al., "Fault-tolerant control for multiple open-leg faults in open-end winding permanent magnet synchronous motor system based on winding reconnection," *IEEE Transactions on Power Electronics* 36(5), 6068–6078, 2020.

[81] A. Ghaderi, "Motor control method, power conversion device, motor module, and electric power steering device," Patent No. US 11,031,880 B2, June 8, 2021.

[82] A. Ghaderi, "Motor control method, power conversion device, motor module, and electric power steering system," Patent No. US 11,031,880 B2, June 2, 2020.

[83] R. Xiong, et al., "A sensor fault diagnosis method for a lithium-ion battery pack in electric vehicles," *IEEE Transactions on Power Electronics* 34(10), 9709–9718, 2019.

[84] L. Yao, et al., "Fault Identification of Lithium-Ion Battery Pack for Electric Vehicle Based on GA Optimized ELM Neural Network," *IEEE Access* 10, 15007–15022, 2022.

[85] R. Yang, R. Xiong, and W. Shen, "On-board soft short circuit fault diagnosis of lithium-ion battery packs for electric vehicles using extended Kalman filter," *CSEE Journal of Power and Energy Systems* 8(1), 258–270, 2022.

[86] Tim Burress," Electrical performance, reliability analysis, and characterization", *2017 United States DoE, Vehicle Technologies Offices, Annual Merit Review*. [Online] available at: https://www.energy.gov/eere/vehicles/articles/vehicle-technologies-office-merit-review-2017-electrical-performance.

[87] Electrical and electronics technical team roadmap, *US. DRIVE, US Department of Energy, Vehicle Technologies Office*, October 2017. [Online]:https://www.energy.gov/sites/prod/files/2017/11/f39/EETT%20Roadmap%2010-27-17.pdf.

Babak Fahimi (S'96-M'99-SM'03-F'15) earned his PhD degree from Texas A&M University, College Station, TX in 1999. After spending 3 years at Electro Standards Laboratories Inc. in Rhode Island as a research scientist, he started his academic career in 2002. Dr. Fahimi has since supervised 36 PhD and 24 M.S. theses to successful completion, has co-authored over 380 scientific articles and has 22 issued and six pending patents to his credit. Dr. Fahimi has been the principal investigator of several successful research programs funded by ARPA-e, ONR, NSF, and DoE as well as many industrial projects. For his excellence in research and education he has been recognized with the Richard M. Bass young power electronics investigator award from IEEE-PELS in 2003, Cyril Veinott electromechanical energy conversion award from the IEEE-P&E in 2015, and Ralph Teetor educational award from the society of automotive engineers in 2008. Dr. Fahimi is a distinguished chair of engineering at UT-Dallas and is a Fellow of IEEE for his contributions to the modeling and analysis of AC adjustable speed drives. His areas of interest include optimal design and control of adjustable speed drives, design and development of high-performance power converters, and applications of power electronics to clean energy, healthcare, and electrified transportation.

Laura H. Lewis (F'22) is the Distinguished University and Cabot Professor of Chemical Engineering and Professor of Mechanical and Industrial Engineering at Northeastern University in Boston, MA. Her research focuses on investigating the materials factors at the atomic level that provide functionality to magnetic and electronic materials, with particular expertise in advanced permanent magnets. She has participated on a number of advisory panels and currently serves on the Scientific Advisory Board of the Critical Materials Institute (a DOE Energy Innovation Hub) and is a member of the U.S. Technical Advisory Groups to develop supply chain and sustainability standards as a US Delegate to ISO TC298 (Rare Earths) and ISO TC333 (Lithium), American National Standards Institute (ANSI). Laura is a Fellow of the IEEE and was Conference Editor of the *IEEE Transactions on Magnetics* (2008 – 2018) and Chair of the IEEE Magnetics Society Technical Committee (2017-2019). She is a Fellow of the American Physical Society, a Fulbright Fellow as well as a member of JEMS-EMA (The European Magnetism Association), the Materials Research Society, the American Chemical Society and the American Society for Engineering Education.

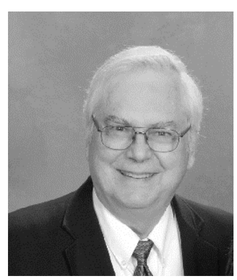

John M. Miller (S'74-M'76-SM'94-F'99-LF'16) is owner and founder of J-N-J Miller Design Services PLLC, which was established in 2002 to provide professional consulting in conductive/wireless charging, electrochemical energy storage systems, hybrid electric vehicle propulsion systems, and vehicle electrification. Dr. Miller has over 47 years of experience in electrical engineering across various industries that include automotive electrical systems, electric traction drive systems, aerospace/military guidance systems, white goods microprocessor control, and electrical practice in residential/commercial/industrial installations. He was senior scientist for Momentum Dynamics Corp (now InductEV), distinguished R&D scientist at Oak Ridge National Laboratory (ORNL) where he held positions as Director of the Power Electronics and Electric Power Systems Research Center, and Program Manager of the DoE Vehicular Technologies subprogram APEEM. Prior to ORNL, he held various engineering and senior management positions at

Maxwell Technologies as VP, Ford Motor Company, and Texas Instruments. Dr. Miller has published several books related to wireless charging, ultracapacitor applications (including Chinese edition), propulsion systems for hybrid vehicles (1st and 2nd editions plus translated into Chinese), automotive power electronics, and vehicular electric power systems. He holds a B.S.E.E. from the University of Arkansas-Fayetteville, M.S.E.E. from Southern Methodist University, Dallas, TX, and Ph.D. from Michigan State University, East Lansing, MI. Dr. Miller is a Life Fellow of the IEEE and Fellow of the SAE and a registered professional engineer in Michigan (1980) and Texas (2014).

Steven D. Pekarek (M'91-F'13) received his PhD in electrical engineering from Purdue University in 1996. From 1997-2004 Dr. Pekarek was an assistant (associate professor of electrical and computer engineering at the University of Missouri-Rolla (UMR). He is presently the Edmund O. Schweitzer III professor of electrical and computer engineering at Purdue University. He is an active member of the IEEE power engineering society, the electric ship research and development consortium (ESRDC), and the advancing sustainability through powered infrastructure for roadway electrification (ASPIRE) center. He has served as the technical chair of the 2007 IEEE applied power electronics conference (APEC) and technical chair of the 2013 IEEE electric machines and drives conference (IEMDC). He has also served as an editor for the IEEE Transactions on Energy Conversion.

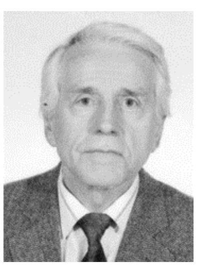

Ion Boldea (F'96, LF'12) studied and published extensively on “rotary and liners electric machines, drives and MAGLEVs design ,control and testing for energy saving and increased productivity in various industries: from renewable energy, through e-transport, robotics, industrial drives, home appliances and info-gadjets since 1976(ISI H-index 41(4173 citations),Scopus H-index 49(8202 citations),Google Academic H-index 61(6246 citations); he wrote more than 20 Monographs and textbooks in USA and U.K on the wide spectrum subjects above (6000 citations in World.cat), held IEEE DLs since 2008, intensive Courses in USA, EU,S. Korea, Brazil, China , tutorials at IEEE Conferences, Technical Consulting annual contracts, hosted IEEE Trans. special issues and spent more than 5 years in many visits since 1973 as visiting scholar in USA. He supervised 24 Ph.D. students successfully. He received “IEEE 2015 Nikola Tesla Award” and “2021 EPE-ECCE Outstanding Achievement Award”.

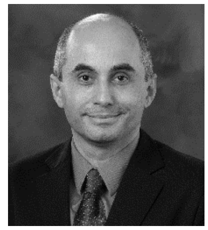

Burak Ozpineci (S'92-M'02-SM'05-F'20) received the B.S. degree in electrical engineering from Orta Dogu Technical University, Ankara, Turkey, in 1994, and the M.S. and Ph.D. degrees in electrical engineering from The University of Tennessee, Knoxville, TN, USA, in 1998 and 2002, respectively. In 2001, he joined the Post-Master's Program with Power Electronics and Electric Machinery Group, Oak Ridge National Laboratory (ORNL), Knoxville, TN, USA. He became a Full Time Research and Development Staff Member in 2002, the Group Leader of the Power and Energy Systems Group in 2008, and Power Electronics and Electric Machinery Group in 2011. Presently, he is a Corporate Fellow at ORNL serving as the Section Head for the Vehicle and Mobility System Research Section. He is also a Joint Faculty with the Bredesen Center, The University of Tennessee. Dr. Ozpineci is a Fellow of IEEE and AAIA.

Kay Hameyer (M'96-SM'99) received his M.Sc. degree in electrical engineering from the University of Hannover and his Ph.D. degree from the Berlin University of Technology, Germany. After his university studies he worked with the Robert Bosch GmbH in Stuttgart, Germany as a Design Engineer for permanent magnet servo motors and vehicle board net components. Until 2004 Dr. Hameyer was a full Professor for Numerical Field Computations and Electrical Machines with the KU Leuven in Belgium. Since 2004, he is full professor and the director of the Institute of Electrical Machines (IEM) at RWTH Aachen University in Germany. From 2006 on he served as vice dean and from 2007 to 2009 he was elected dean of the faculty of Electrical Engineering and Information Technology of RWTH Aachen University. His research interests are numerical field computation and optimization, the design and controls of electrical machines, in particular permanent magnet excited machines and induction machines. Since several years Dr. Hameyer's work is concerned with the characterization and modelling of soft- and hard-magnetic materials to enhance the performance of electric drive systems. Own developments of measurement technology for winding insulation systems for high du/dt inverter fed operated low voltage electrical machines leads to models for the life-time estimation of insulation systems. Magnetically excited audible noise in electrical machines are further topics of interest. Dr. Hameyer is author of more than 350 journal publications, more than 700 international conference publications and author of 4 books. Dr. Hameyer is a member of VDE, IEEE senior member and fellow of the IET.

This article has been accepted for publication in IEEE Transactions on Transportation Electrification. This is the author's version which has not been fully edited and content may change prior to final publication. Citation information: DOI 10.1109/TTE.2023.3321707

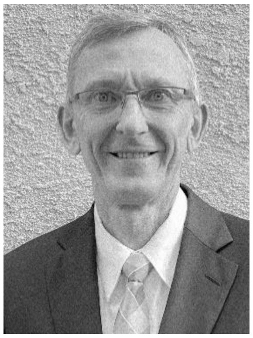

Steven E. Schulz (S'88-M'90-SM'02) obtained the M.S. degree in Electrical Engineering from Virginia Tech in 1991 and has been working in the field of power electronics for over 32 years. He has worked on EV and HEV systems since 1992, including such landmark vehicles as General Motors EV1, Chevrolet Volt, and Rivian R1T. Mr. Schulz has also spent several years in the aerospace industry working on satellite applications, including power distribution, conversion, and electric propulsion. He previously held the position of Technical Fellow with General Motors until 2013, specializing in power electronics and motor control. From 2014-2018 he was a Technical Fellow with Faraday Future developing high power electronics for their vehicles. He is currently Director of Electrical Design for the Electric Power Conversion group at Rivian Automotive, developing propulsion and charging solutions.

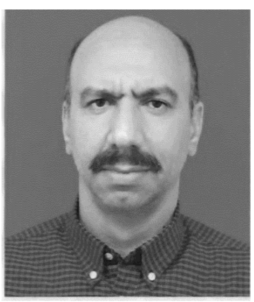

Ahmad Ghaderi (M'08) earned his B.S., M.S., and Ph.D. in Electrical Engineering from Shahed University, Iran, Isfahan University of Technology, Iran, and Kyushu Institute of Technology, Japan, in 1999, 2002, and 2007, respectively. He began his career at the National Iranian Oil Refining and Distribution Company from 2002 to 2003, followed by a role as a Research Assistant at Japan's Robotics Research Institute from 2004 to 2006. In 2007-2008, he served as a Researcher at the Kyushu Institute of Technology, Japan. From 2008 to 2011, he worked at the HV Electric System Lab, Toyota Central R&D Labs, Inc., Japan. From 2011 to 2018, Ahmad Ghaderi contributed to the Research and Development Department of Nidec Corporation in Japan and the U.K. Subsequently, from 2018 to 2021, he held the position of System Technical Project Lead at Continental Automotive Hybrid Electric Vehicles Business Unit and Vitesco Technologies in Dearborn, Michigan. Currently, he serves as the Chief System Engineer in the Commercial Vehicle Engineering department at Dana Incorporated in Novi, Michigan. His research interests encompass motor drive systems and electric drive vehicle propulsion systems.

Mircea Popescu (M '98-SM'04- F '15) is Principal Product Specialist with Ansys UK. He received the M.Eng. and Ph.D. degrees in electrical engineering from the "Politehnica" University of Bucharest, Romania, and the D.Sc. (Tech) degree in electrical machines from Aalto University, Espoo, Finland.

He has 40 years of experience in research & development and academic teaching focused on electrical machines and drives. Earlier in his career, he was with National Research Institute for Electrical Engineering, Bucharest, Romania, Helsinki University of Technology (now Aalto University), Finland, SPEED Lab at University of Glasgow, U.K. and Motor Design Ltd, U.K. He has published more than 200 peer reviewed papers with more than 7000 citations and his publications have received three IEEE best paper awards. An IEEE Fellow, Dr. Popescu is Associate Editor for IEEE Transactions on Industry Applications and IET Electric and Power Applications journal. He served as an Officer of the IEEE Industry Application Society Electrical Machines Committee 2010 – 2017 and Prominent Lecturer for IAS Region 8, 2014-2016.

Brad Lehman (M'92-SM'08-F'20) is a professor of electrical engineering at Northeastern University. He is President of the IEEE Power Electronics Society (PELS, 2022-2023). He previously was Editor-in-Chief of the IEEE Transactions on Power Electronics from 2013-2018. Dr. Lehman has been the recipient of the 2015 IEEE (PELS) Modeling and Control Technical Achievement Award, a 2016 IEEE Standards Medallion, the 2018 IEEE Award for Achievement in Power Electronics Standards, and the 2019 IEEE PELS Harry A. Owen, Jr. Distinguished Service Award. He has been listed in the inaugural edition of the book *The 300 Best Professors*, Princeton Review, 2012. He performs research in power electronics and renewable energy.

Dhruvi Patel (S' 22) was born in Ahmedabad, India. She received the B.Tech. degree from the LD College of Engineering, Ahmedabad, India, in 2016 and M. Tech. degree from LD Institute of Technology and Research, Gandhinagar, India in 2019. She joined the Renewable Energy and Vehicular Technology Laboratory at the University of Texas at Dallas, Richardson, TX, USA, in 2021. Her area of research is electric drives and e-mobility.